AD NUMBER
AD842030
LIMITATION CHANGES
TO: **Approved for public release; distribution is unlimited.**
FROM: **Distribution: Further dissemination only as directed by Air Force Space and Missile Systems Organization, SMSD, Norton AFB, CA, MAY 1968, or higher DoD authority.**
AUTHORITY
samso, usaf ltr, 28 feb 1972

SAMSO TR 68-362 VOL II

SEMIANNUAL PROGRESS REPORT

ADVANCED PENETRATION PROBLEMS

WAKE STRUCTURE MEASUREMENTS

A. Demetriades
Space and Re-Entry Systems
Division of Philco-Ford Corporation

15 May 1968

Space and Missile Systems Organization
Air Force Systems Command
Norton Air Force Base, California

(9) SEMIANNUAL PROGRESS REPORT. 16 Oct 67 - 15 Apr 68,

(6)

ADVANCED PENETRATION PROBLEMS

WAKE STRUCTURE MEASUREMENTS.

(10) A. Demetriades
Space and Re-Entry Systems
Division of Philco-Ford Corporation

(18) SAMSO (19) TR-68-362-Vol-2

(11) 15 May 1968

(12) 610.

(15) F04701-68-C-0032, ARPA Order-888

Space and Missile Systems Organization
Air Force Systems Command
Norton Air Force Base, California

FORWARD

(U) This Semiannual Progress Report by Philco-Ford, Space and Re-entry Systems Division, Newport Beach, California, on the Advanced Penetration Problems Task of Wake Structure Measurements was prepared for the Advanced Research Projects Agency, Department of Defense, ARPA Order No. 888. The research was monitored by the Space and Missile Systems Organization, USAF under Contract F04701-68-C-0032.

(U) The author is Dr. A. Demetriades of Philco-Ford, Space and Re-entry Systems Division. The data herein covers the reporting period of 16 October 1967 through 15 April 1968.

(U) This technical report has been reviewed and is approved.

W. D. McComb
Advanced Penetration Problems
Project Officer

ABSTRACT

(U) Progress on the subject contract in the period October 15, 1967 to April 15, 1968 is described in this report. Work has been performed on the turbulent structure of a two-dimensional supersonic wake at angle of attack, on a similar wake at zero incidence but with heat transfer, and a turbulent plasma jet. Data from a zero-incidence, adiabatic wake are being further reduced. Notable findings in these experiments include highly accurate values of the turbulent Reynolds and Prandtl number, a re-appearance of the so-called front wavelength of free turbulence, and the explanation of very large electron density fluctuations as due to transitional mixing.

BLANK PAGE

CONTENTS

SECTION		PAGE
I	SUMMARY OF WORK	1
II	STRUCTURE OF THE TWO-DIMENSIONAL WAKE	3
	2.1 Introduction	3
	2.2 Mean Flow in the Two-Dimensional Wake.	3
	2.3 Intermittency.	7
	2.4 The Turbulent Flow	11
III	THE TURBULENT PLASMA JET	15
	3.1 The Intermittent Flow.	15
	3.2 The Large Electron Density Fluctuations. . . .	25
IV	SUPERSONIC WAKES AT ANGLE OF ATTACK	32
	4.1 Introduction	32
	4.2 Model and Facilities	32
	4.3 Experiment Design.	33
	4.4 Diagnostic Instrumentation	39
	4.5 Procedure.	39
	4.6 Results of Measurements.	39
V	SUPERSONIC WAKE WITH HEAT TRANSFER	45
	5.1 Introduction	45
	5.2 Model and Facilities	45
	5.3 Adjustment of Operating Conditions	46
	5.4 Procedures and Instrumentation	48
	5.5 Results to Date.	49
	REFERENCES.	53

ILLUSTRATIONS

FIGURE		PAGE
1	Variation of Two-Dimensional Wake Momentum and Energy Thickness.	5
2	Radial Variations of Non-Dimensional Wake Velocity (Top) and Ambient Temperature (Below)	6
3	Axial Variations of Turbulent Reynolds Number From the Two-Dimensional Wake	8
4	Axial Variation of the Mean Front Position and Its Standard Deviation.	9
5	Non-Dimensional Forms of the Front Position and Standard Deviation Comparing These Lengths with the Transverse Scale.	10
6	Unresolved Spectra of Turbulence at a Fixed Point in the Wake, Illustrating the Effect of Response Restoration (Proper Frequency Response)	13
7	Restored, One-Dimensional, Unresolved Spectra at Fixed Radial but Varied Axial Positions	14
8	Variation of Intermittency Factor in the Jet, Compared with Typical Temperatures and Electron Density Distributions	17
9	Growth of the Boundary Enveloping the Fully Turbulent Jet Fluid.	18
10	The Turbulent Jet Front Position and Its Standard Deviation	19
11	Distribution of the Intermittency Factor and Null-Crossing Frequencies About the Front Position . . .	20
12	Variation of the Null-Crossing Frequencies with Distance.	21
13	Variation of Front Wavelength of Typical Free Turbulent Flows	23
14	Comparison of Turbulent Front Growth with Typical Low-Speed Data.	24

ILLUSTRATIONS (Continued)

FIGURE		PAGE
15	Variation of Normalized Electron Density Fluctuations Along the Jet Axis	26
16	Oscilloscopic Study of Temperature and Electron Density Fluctuations.	27
17	Reconstructed "Snapshot" of the Distribution of Electron Density Along the Jet	30
18	Photograph of Wind-Tunnel Test-Section Showing Two-Dimensional Model Support	34
19	Schematic of Two-Dimensional Wake Nomenclature. . .	35
20	Flow-Field in the Wake of the Two-Dimensional Body at 20-Degree Incidence, From Characteristics Calculation	36
21	Flow Properties at Fixed Distances Behind the Model at 20-Degree Incidence.	37
22	Theoretical and Experimental Deduction of Flow Properties in the Wake.	40
23	Typical Pitot-Probe Traces of the Two-Dimensional Wake at Various Angles of Attack.	42
24	Typical Static-Probe Traces of the Two-Dimensional Wake for a 20-Degree Incidence Angle.	43
25	Delay of Transition to Turbulence in the Wake Brought About by Heat Transfer.	47

SECTION I

SUMMARY OF WORK

Reduction of data has continued on the two-dimensional turbulent wake at zero incidence and heat-transfer. Evaluation of the wake drag and energy integrals along the stream direction showed that these were constant with distance, meaning that the experiment had been "tailored" properly. The virtual diameter was such that a wake "map" to almost 2,000 diameters became possible. Similarity in the radial direction was demonstrated by a very consistent collapse of the data on the same curve. The expected agreement with low-speed data in the far wake was shown, and, in fact, the turbulent Reynolds number was found to be 13.0. The matter of this number, important to the hypersonic wake, should be considered fairly settled by this time. In the turbulence aspect, the presence of the "front wavelength" was again detected, bearing apparently the same geometric similarity to the wake diameter as was found in the axisymmetric wake.

The effects of angle of attack and heat-transfer on the wake structure, long suspected to be decisive, have been for the first time tackled in comprehensive laboratory studies. These are performed with two-dimensional geometries as a logical first step to introducing gradually the complexities of the final problem. The experiments are now nearly complete, although the data have not been reduced. Nevertheless at least one important prediction of the Lees-Gold stability theory, the delay of transition when the wake is stabilized by heating, has been verified.

Further information has emerged from the data reduction sequence of the turbulent plasma jet experiment. It is now known that the front (interfacial) structure of the jet has the same geometric features for an electron-sensitive observer that it does, say, for a temperature-sensitive observer. The longitudinal wavelength by which this structure is organized is, apparently, obeying the same relation to the jet diameter that the wake-front scale bears to the wake diameter. In the zone of jet transition-to-turbulence the mixing process has been found to resemble, to some extent, the speculative models advanced early in this decade by Lin and Proudian. Once the transition process is complete, and for recombination reaction rates which are apparently too slow for the turbulence, the electron density fluctuation approach numerically the fluctuations in the gas density. The integral scales of electron density fluctuations do not appear to scale directly with the jet diameter as expected for the scales of neutral gas variables. This significant point is being pursued further.

During the past six months an effort has been made to review the present experiments critically in the light of work done in other laboratories, to document the present findings into the form of technical reports, and to disseminate unclassified portions to the technical community at large in the hope of eliciting critical comments. Technical exchanges have been held with the Caltech group under Prof. L. Lees and the group at AC Electronics working with Dr. K. S. Wen. In the course of technical presentations by RCA/Canada at

SAMSO, Philco-Ford personnel had the opportunity of evaluating experiments related to the Philco-Ford work. In April 1968 A. Demetrades visited CARI in Quebec, Canada, and examined at close quarters the work done in the ballistic range at speeds of 15,000 fps. A technical report was written in February 1968 on the mean flow properties of the turbulent jet; two earlier papers dealing with basic aspects of wake structure have been accepted for publication in the Physics of Fluids Journal and the Journal of Fluid Mechanics, and a third paper dealing with the intermittency properties of the turbulent jet has been approved for delivery at the Fluids and Plasmas Conference of the AIAA in June 1968 in Los Angeles, Calif. On April 25, 1968, A. Demetriades delivered a talk entitled "Structure of Compressible Turbulent Wakes" at the 12th AMRAC meeting in Washington, D. C. This paper will appear in the AMRAC Proceedings which will be available shortly.

SECTION II

STRUCTURE OF THE TWO-DIMENSIONAL WAKE

2.1 INTRODUCTION

The two-dimensional wake work (WED experiment) completed during the previous contract period is yielding a wealth of important information through a continued program of data reduction and interpretation. In Reference 1 detailed information on this experiment is supplied as regards the facilities, model, instrumentation and procedures, and the preliminary evaluation of the mean and turbulent flow raw data. In the present Section the final results as regards the mean and intermittent flow will be outlined; the turbulence results will be described at the present reduction stage.

2.2 MEAN FLOW IN THE TWO-DIMENSIONAL WAKE

2.2.1 ANALYSIS

A similarity analysis of the two-dimensional compressible turbulent wake has been carried out along lines similar to those for the axi-symmetric wake (Reference 2). As in all similarity analysis of comparable flows, the analysis utilizes at least one empirical fact, namely that the axis velocity decays as the inverse-square of axial distance. With this input, the results are that the axis temperature defect also decays as $1/\sqrt{x}$, and that the density defect decay approaches the $1/\sqrt{x}$ behavior much later than either the velocity or the temperature. The transverse scale L increases as $\sqrt{x}$, and the radial profiles of velocity and temperature are similar in the radial parameter $\tilde{Y}/L$ where $\tilde{Y}$ is the Howarth-Dorodnitzyn radius.

Quite recently Laufer (Reference 3) has given a formal procedure for deriving the characteristics of mean compressible turbulent (free) flows once the corresponding incompressible flow is known.* His results are nearly identical to those outlined in the previous paragraph and give the following relation for the axis velocity defect far in the wake:

$$w \equiv \frac{u_\infty - u(o)}{u_\infty} = \sqrt{\frac{R_T}{10}}\,\frac{1}{\sqrt{\bar{x}}} \qquad (1)$$

where u and u(o) are (in the wind-tunnel coordinate) the velocity just external on the wake and on the axis respectively, R_T is the Turbulent Reynolds Number and where x accounts for the virtual origin x_o and the two-dimensional drag C_Dh:

$$\bar{x} \equiv \frac{x - x_o}{C_D h} \qquad (2)$$

*D. J. Laufer, head of the Department of Aerospace Engineering at the University of Southern California, is a Philco-Ford Consultant.

It is furthermore predicted that the factor in the Gaussian exponent of the velocity distribution is 0.5, that is

$$\tilde{u} = \frac{u_\infty - u}{u_\infty - u(o)} = e^{-\frac{\eta^2}{2}} \qquad (3)$$

where $\eta \equiv \tilde{Y}/L$.

It should be noted that the similarity law $w \sim \bar{x}^{-1/2}$ differs in the exponent in the corresponding law for the axi-symmetric wake, $w \sim \bar{x}^{-1/3}$. The target of this subtask is therefore primarily the existence of similarity and especially the value of R_T which is equally important to the axi-symmetric wake as well and which is expected to be insensitive to geometry.

2.2.2 RESULTS

Reference 1 presented experimental results from WED as already reduced thru the WEB-I (DR 25F) program. In that program quantities at various radial positions were outputed as a function of radius divided by the so-called half-radius of the wake. This type of presentation is a rather insufficient test of similarity, since it forces all points to pass through too many points - it forces, that is, data at various stations to collapse on a single curve regardless of similarity. A new program, WEB-VIII (SRS No. 0064), was therefore composed whose main function was to re-normalize the radius so that quantities could be plotted versus $\eta \equiv \tilde{Y}/L$. The new program also outputs the normalized physical radius Y/L, the integrals of momentum (i.e. C_{Dh}) and energy, the average value of C_{Dh} and the quantity $\bar{x}$, the wake Reynolds Number Re_w and so on.

The energy integral and the momentum integral should be constant along a wake which is unaffected by drag "swallowing", that is for a wake which, as the present experiment intended, possesses only an insignificant shock signature. Figure 1 shows that indeed this is the case. The average C_{Dh}, computed by excluding the first few points which are obviously affected partly by instrument resolution is 0.00909 cm. This length can be thought of as the effective frontal height of a two-dimensional body of drag coefficient of unity. It is not coincidental perhaps that the actual frontal height of the ribbon is 0.01 cm, within 10 percent of that figure.

The radial distributions of velocity and temperature are shown on Figure 2 as plotted versus η. The correlation is quite satisfactory. It is especially significant that the velocity data $\tilde{u}$ pass through the point ($\tilde{u} = 0.5$, $\eta = 1$) quite unaided, signifying a near-equality of the scale L and the half-radius. The similarity distribution for $\tilde{u}$ and $\tilde{T}$:

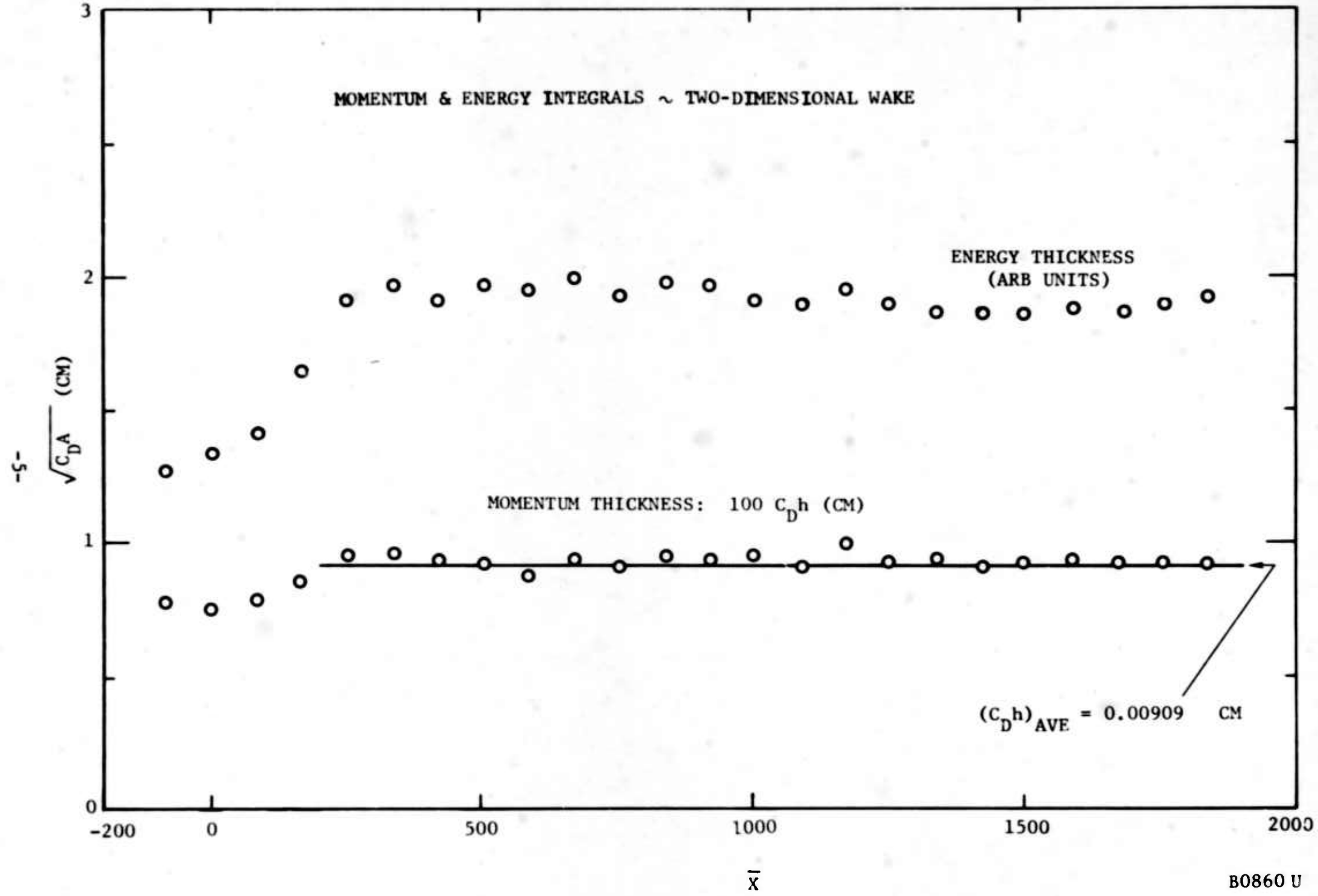

FIGURE 1 VARIATION OF TWO-DIMENSIONAL WAKE MOMENTUM AND ENERGY THICKNESS

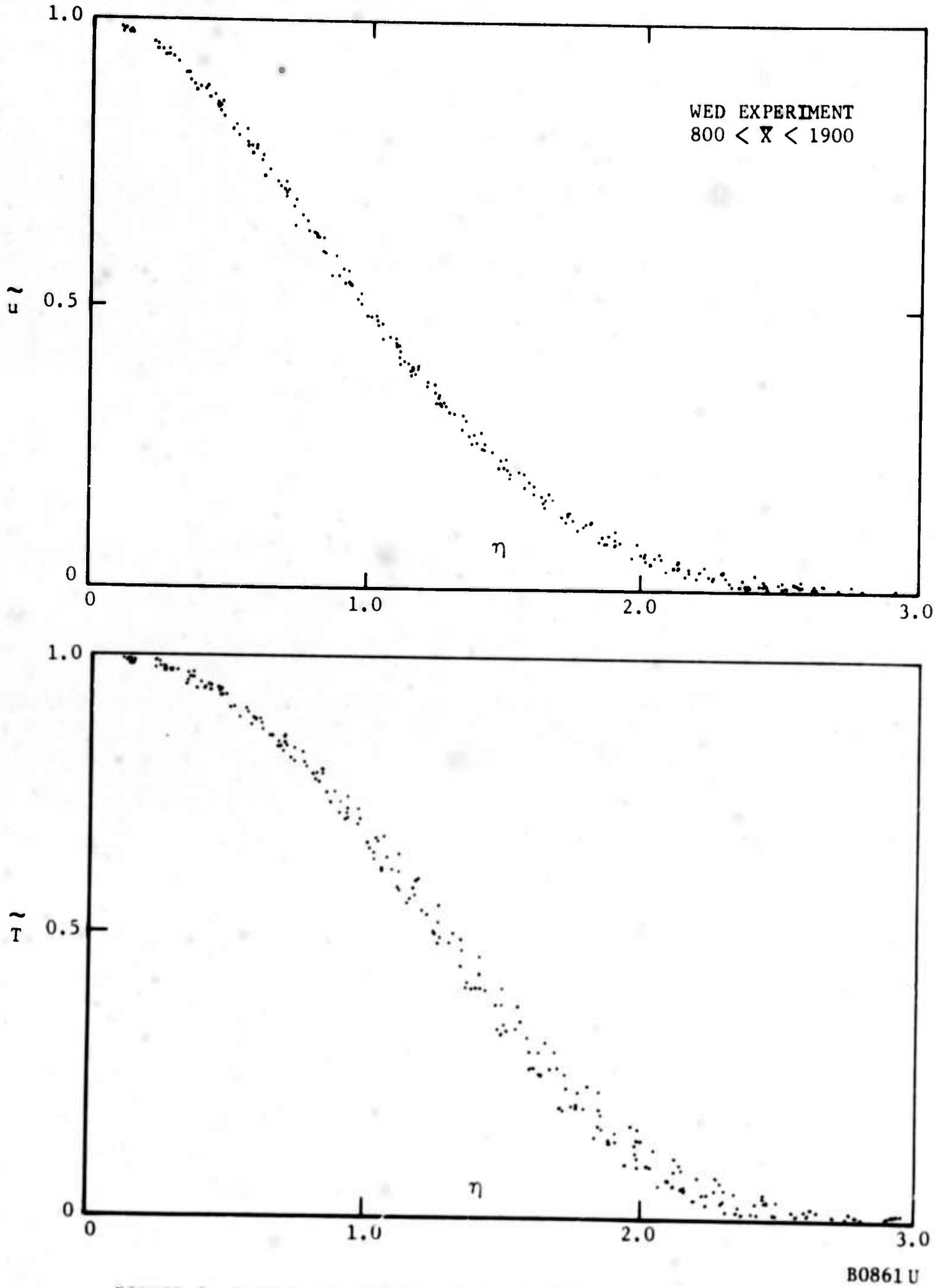

B0861U

FIGURE 2 RADIAL VARIATIONS OF NON-DIMENSIONAL WAKE VELOCITY (TOP) AND AMBIENT TEMPERATURE (BELOW)

$$\tilde{T} \equiv \frac{T - T_\infty}{T(o) - T_\infty} \tag{4}$$

is Gaussian in character.

The axial variations of the scale L and of the defects have already been presented in Figures 34, 35 and 36 of Reference 1. Since the abscissa XSTATION of these figures is simply proportional to the correct axial parameter $\bar{x}$, it is indeed seen that $L \sim \sqrt{\bar{x}}$ and $w, \theta \sim \bar{x}^{-1/2}$ as expected. We can now present, in addition, the value of the Reynolds Number R_T as obtained from the present experiment. Using equation (1):

$$R_T = 10\, \bar{x}\, w^2 \tag{5}$$

we obtain the results shown on Figure 3. The average value (again excluding a short distance near the body) is 13.0, remarkably close to the 12.7 found by Tounsend at low speeds (Reference 4) and to the 12.8 found for the supersonic aci-symmetric wake (Reference 2).

The identity among these numbers is of course hardly surprising in view of the fact that all wake flows eventually decelerate to the speed of the ambient environment. Intense compressibility effects cannot be extracted from the present experiment. In fact spot-checks of the effect of plotting the radial variations versus the physical radius Y/L (rather than the $\tilde{Y}$/L) were made. Typically the scatter in Y/L at $\tilde{u} = 0.5$ was about 15 percent of the scatter in $\tilde{Y}$/L - too small an effect from which to draw conclusions.

2.3 INTERMITTENCY

The intermittent properties of the two-dimensional wake have been measured exactly by the same procedure as used for the WEB (see Reference 5). The intermittency factor γ has been found to be distributed normally along the wake radius, i.e., γ is a Gaussian function of radial distance about the position $\bar{Y}$ of the turbulent front. Figure 4 shows the growth of $\bar{Y}$ and of the standard deviation σ with distance; as expected, $\bar{Y}$ and σ are approximately growing as the square root of distance. This growth is shown better in Figure 5, where these two lengths have been normalized by the transverse scale L. The average value of $\bar{Y}$/L is about 1.96, which is only 7 percent than the value obtained for the axi-symmetric wake. However the standard deviation has an average value of about 0.38L, which is considerably lower (by a factor of 2) than the standard deviation of the axi-symmetric wake.

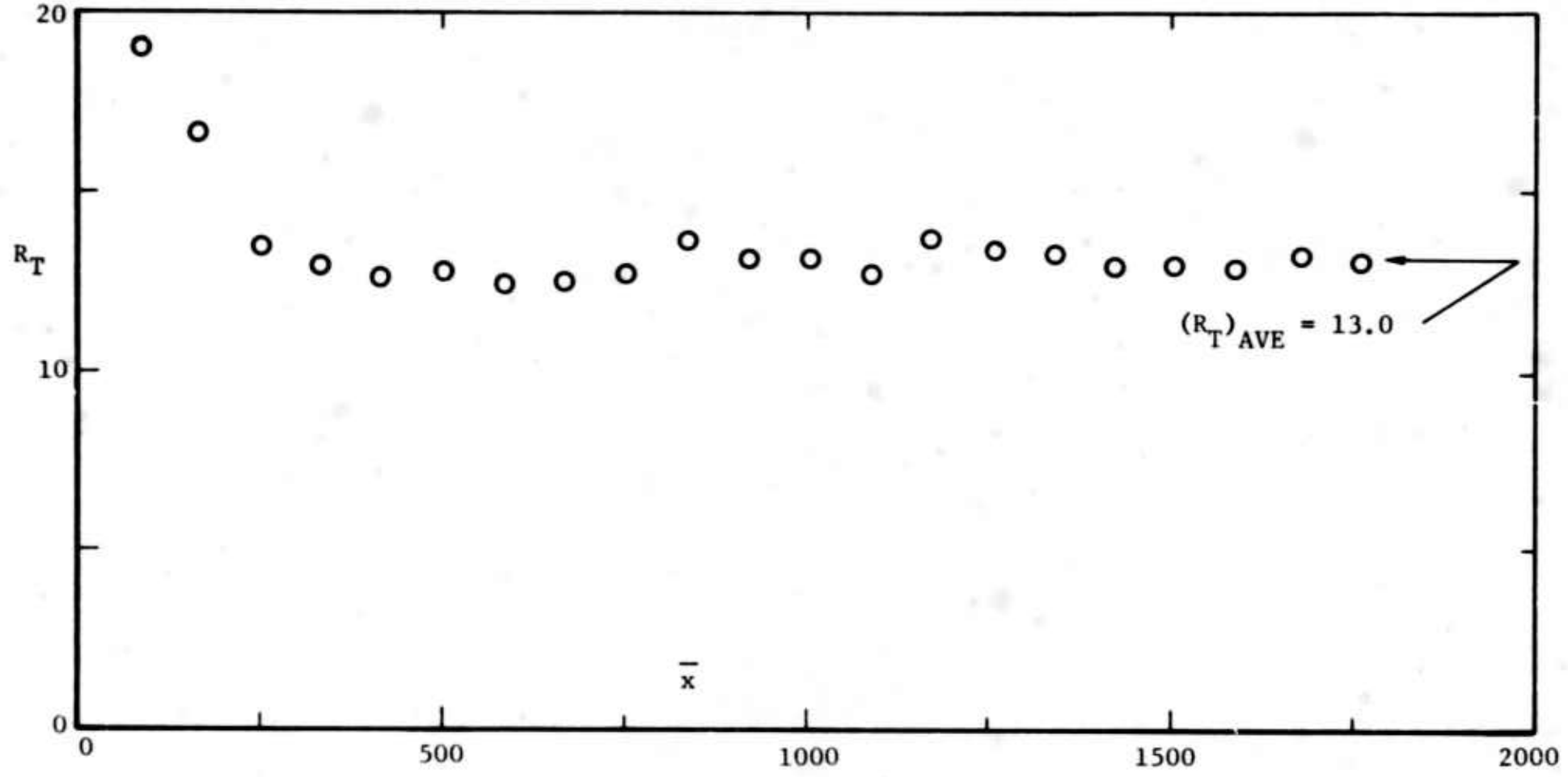

B0862 U

FIGURE 3 AXIAL VARIATIONS OF TURBULENT REYNOLDS NUMBER FROM THE TWO-DIMENSIONAL WAKE

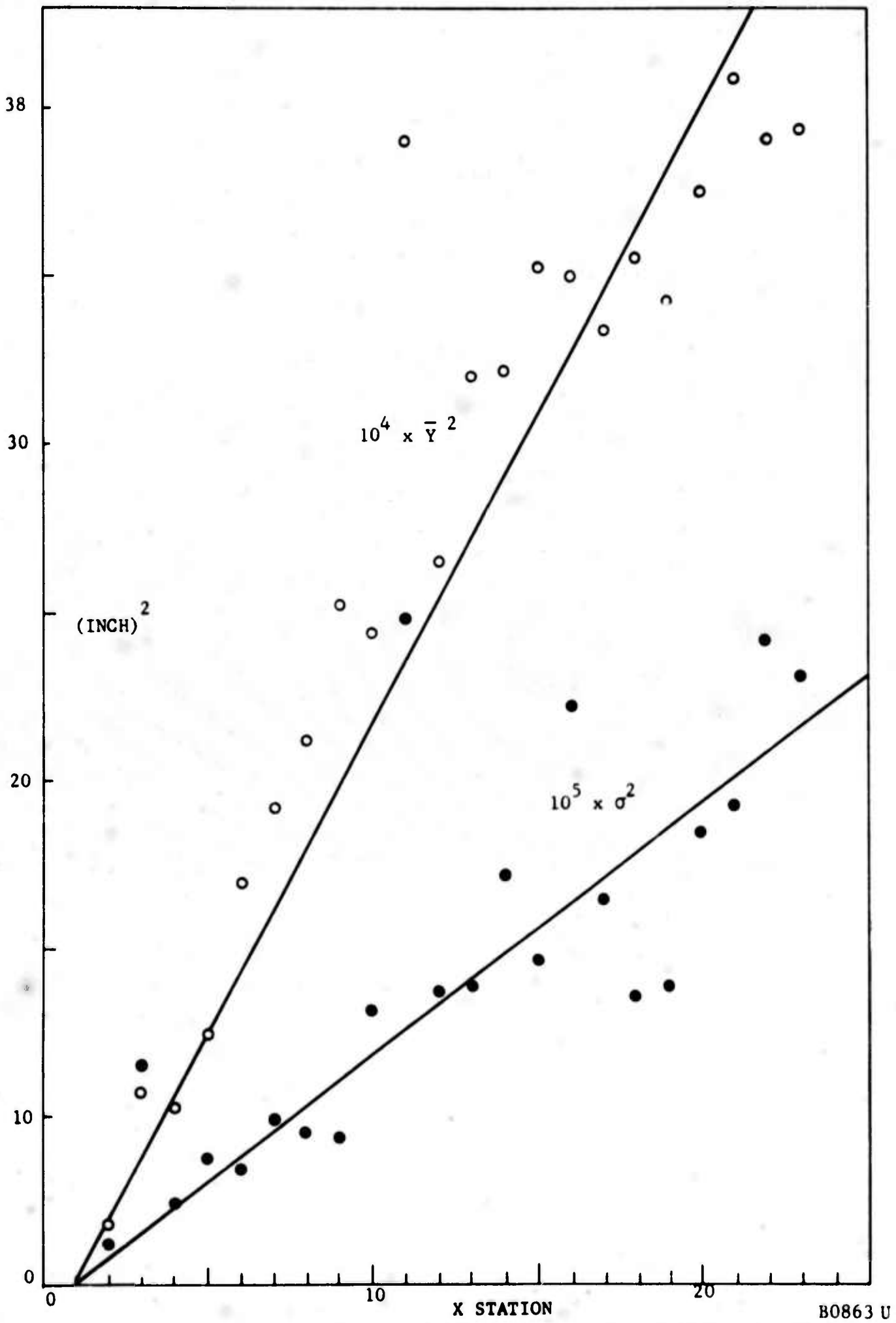

FIGURE 4 AXIAL VARIATION OF THE MEAN FRONT POSITION AND ITS STANDARD DEVIATION

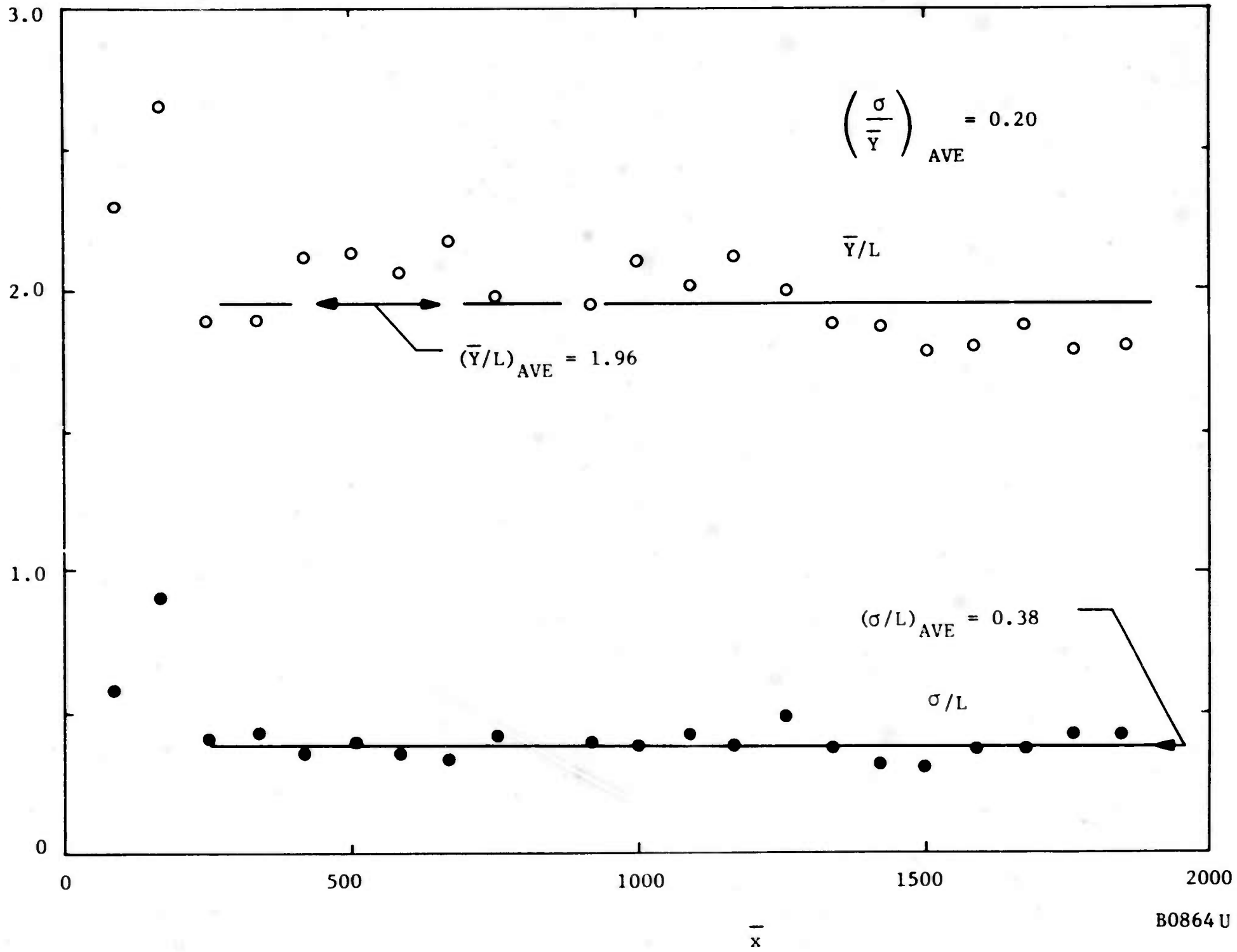

FIGURE 5 NON-DIMENSIONAL FORMS OF THE FRONT POSITION AND STANDARD DEVIATION COMPARING THESE LENGTHS WITH THE TRANSVERSE SCALE

2.4 THE TURBULENT FLOW

In Reference 1 the description of the turbulence flow results obtained with the WEB experiment was limited to the raw data. At this time the reduction of the latter data has progressed through the WEB-II and partly through the WEB-III programs.

The objective of the WEB-II program (Reference 6) is to calculate the response of the overall electromechanical system (including the hot wire) at each frequency passband and to thus produce a numerical factor by which the raw signal in that band is to be corrected. This program then outputs the correct fluctuation spectrum of the wire output, although further resolution of the spectrum into velocity and density contributions (the so-called Modal resolution) occurs later. On the basis of this spectrum, three relevant items will be discussed in this section: the extent of turbulence energy along the spectrum, the differences between uncorrected and corrected spectra and the appearance of the spectral prominence thought to represent the front wavelength.

The Reynolds number of the wake is defined by

$$Re_w = \frac{\left(u_\infty - u(o)\right) L}{\nu_\infty} \qquad (6)$$

where ν_∞ is the kinematic viscosity of the receiving medium. In the two-dimensional wake this number is constant along the wake because the velocity difference $u_\infty - u(o)$ decreases as $\sqrt{x}$ while L increases as $\sqrt{x}$. In the present experiment $Re_w = 158$. Now there is another relevant Reynolds Number, that of turbulence

$$Re_t \equiv \frac{\Delta u \cdot \Lambda}{\nu} \qquad (7)$$

where Δu is rms local velocity fluctuation, Λ the integral fluctuation scale and ν the mean local kinematic viscosity. From the WEA - WEB experiments (Reference 2) it is known that $\Lambda \simeq L$ and that $\Delta u \simeq 0.4 \left(U_\infty - u(o)\right)$ on the wake axis; far in the wake $\nu \simeq \nu_\infty$. As a result the following estimate of Re_t can be made:

$$Re_t = \frac{\Delta u . \Lambda}{\nu} = 0.4 \frac{\left(u_\infty - u(o)\right) L}{\nu} = 0.4\ Re_w \simeq 63 \qquad (8)$$

Furthermore, the stream velocity in the far wake is of the order 60,000 cm/sec and, from the WEB-VIII program, that L is of the order 0.08 cm in the far wake. Thus the frequencies registered by the hot-wire,

as eddies of integral scale size pass it, are of the order 60,000/0.08, that is 750 kilohertz. In turbulence there exist eddies considerably smaller than the integral scale, so that the spectral content being measured should extend into several megahertz.

This highly extended frequency range is too wide to be handled in its entirety by the present hot-wire system. The system, it should be recalled, consists of state-of-the-art componentry, is aided by the forementioned computer program (WEB-II) and it can reliably return results in the range, say, to about 1 MHZ. The net result is that in the present work no attempt was made to go beyond about 1.2 MHZ in the spectra, and the turbulence content for the small-eddy sizes was not measured. However, important features were seen in the range studied, and the frequency-integrated but modally-resolved fluctuations should be correctly deduced since not much energy is anyway contained in the small scales.

With these notations, consider the spectra shown, for example, on Figure 6. The objective here is to consider the effect which the restoration of frequency response effected by the WEB-II program has on the spectral shape. Observe that the response inadequacies of the system without response restoration decreases tremendously the apparent energy content at the higher frequencies. For example in the vicinity of 1 MHZ, the uncorrected spectrum shown is down 100,000 times the zero-frequency value (in the square of spectral density) whereas with proper restoration this decrease is only by a factor of 2. The response-restoration technique thus is crucial to the present experiment.

A final point concerns the peak shown on Figure 6 and more adequately on Figure 7. This sort of energy concentration is, formally speaking, quite unexpected in the one-dimensional spectra of turbulence. Similar peaks were observed, however, in the one-dimensional spectra of the axi-symmetric wake and have already been described in Reference 6. In that work the peak was explained as arising from the periodic structure of the turbulent front which is superposed on the bona fide turbulence spectrum in the region of intense intermittent activity, i.e., away from the axis. If, as shown in Reference 5, this signal has a wavelength related to the wake diameter (or the scale L) one is led to believe that the signal would appear in WED at a much higher frequency, because the WED diameter is much smaller than the WEA diameter. Indeed, the peak frequencies shown on Figure 6 and 7 occur at about 400 KHZ, whereas the peaks in WEA appeared at about 50 KHZ. This ratio of 8 in the wavelength is about equal to the ratio of the axi-symmetric wake diameter to the two-dimensional wake diameter.

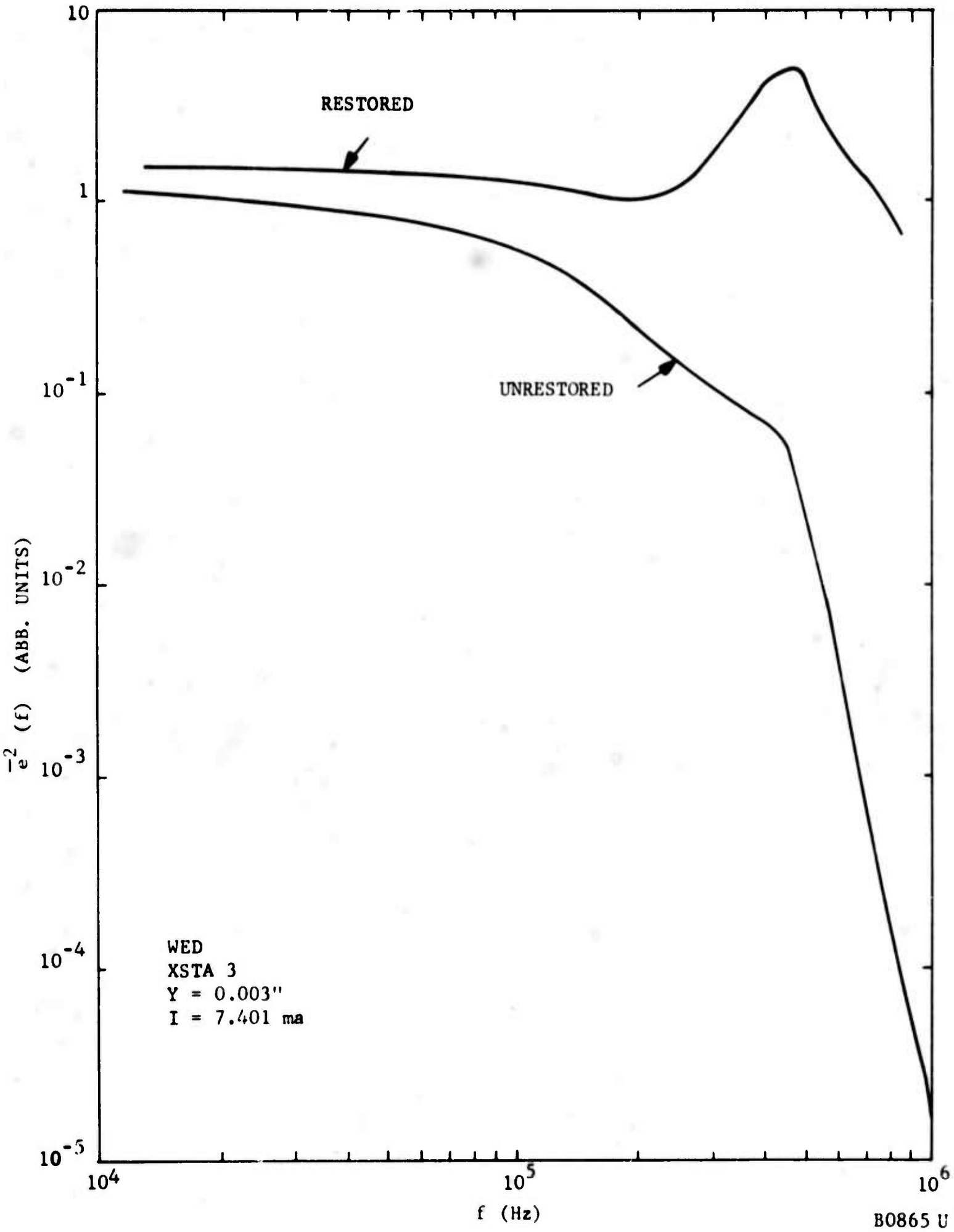

FIGURE 6 UNRESOLVED SPECTRA OF TURBULENCE AT A FIXED POINT IN THE WAKE, ILLUSTRATING THE EFFECT OF RESPONSE RESTORATION(PROPER FREQUENCY RESPONSE)

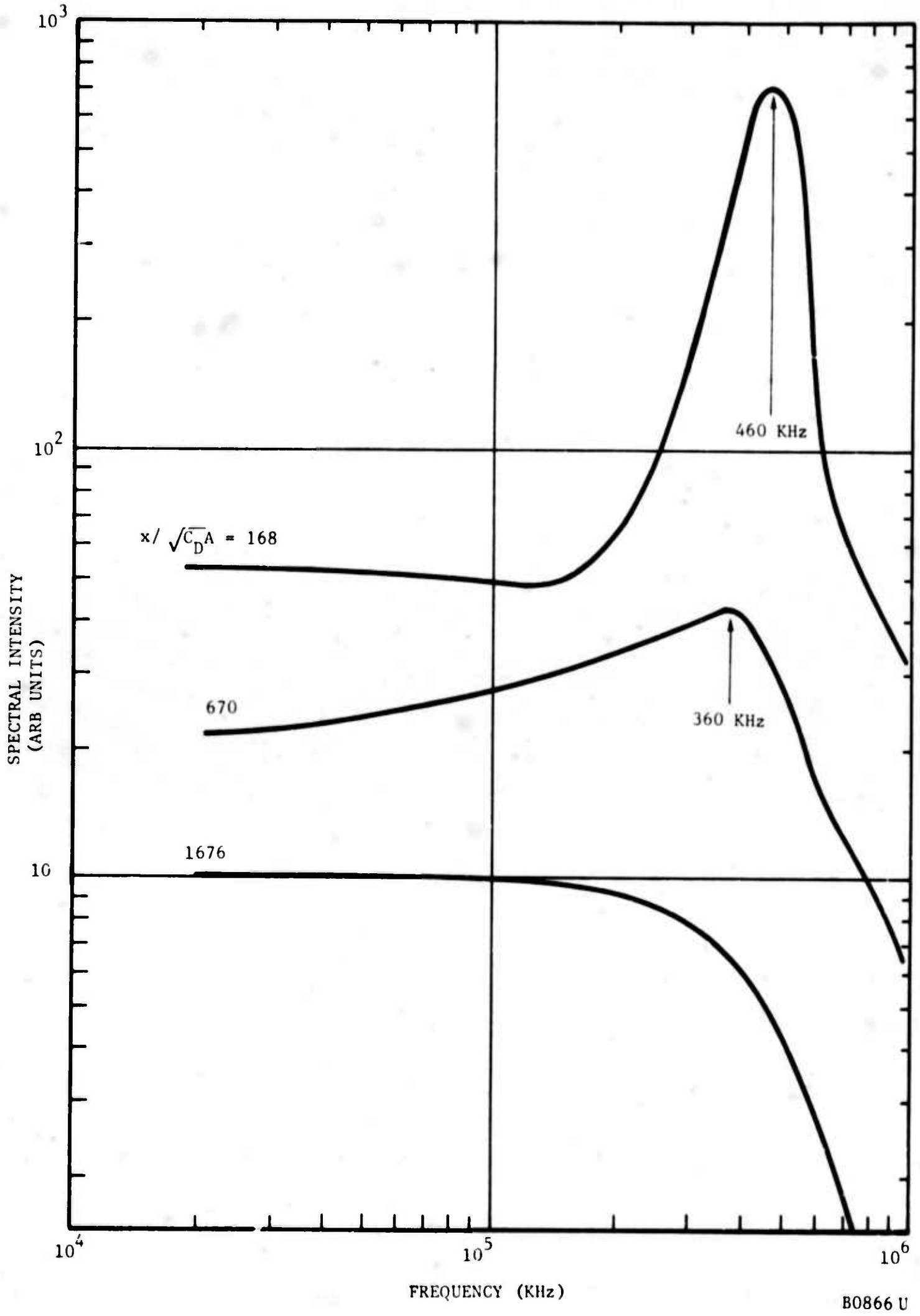

B0866 U

FIGURE 7 RESTORED, ONE-DIMENSIONAL. UNRESOLVED SPECTRA AT FIXED RADIAL BUT VARIED AXIAL POSITIONS

SECTION III

THE TURBULENT PLASMA JET

During the present contract period the work on the mean and intermittent properties of the turbulent argon plasma jet, including the reduction of data, has been completed. Data reduction is proceeding. This section describes in final form the results of the intermittency measurement and the continuing work on the turbulence measurements. The reader is referred to reports from the previous contract period for details on the flow facilities, instrumentation and procedures.

3.1 THE INTERMITTENT FLOW

3.1.1 DEFINITIONS AND PROCEDURES

The measurement of the intermittent flow in the jet is a natural and yet important step in understanding, eventually, the interplay between gas-dynamics and chemistry in the turbulent plasma. As can well be imagined, two important questions arise: (1) how does the high temperatures in the jet affect the statistically averaged geometric features of the front? (2) how does the front geometry and behavior appear to an observer sensitive to the electrons vis-a-vis an observer sensitive, say, to the temperature of the flow?

In the present experiment the front properties were measured with the hot-wire anemometer and the Langmuir probe. The signal from the hot-wire amplifier (or the ac amplifier connected across the load of the Langmuir probe) was fed to the intermittency circuit.

The intermittency factor γ was recorded at each of about 20 radial positions Y at each x. The rms front position $\overline{Y}$ and its standard deviation σ were then obtained from the usual formulas:

$$\overline{Y} \equiv \int_0^\infty Y \frac{d\gamma}{dY}\, dY \tag{8}$$

$$\sigma \equiv \left[\int_0^\infty (Y - \overline{Y})^2 \frac{d\gamma}{dY}\, d(Y - \overline{Y})\right]^{1/2} \tag{9}$$

In these formulas computational convenience requires that γ is expressed as a function of Y. This was done by polynominal-fitting the experimental points with the computer.

In addition to $\bar{Y}$ and σ the autocorrelation scale of the front is of some interest. If the front behaves like a stationary random variable it is possible to find this scale from a measurement of the so-called

null-crossings (or null frequencies) of the front, that is by the frequency $N_o \equiv N(\bar{Y})$ at which a sensor, located at $Y = \bar{Y}$, enters the front. To this end the distribution of null frequencies N(Y) with radius were recorded by electronically counting the rectangular pulses at the Schmidt-trigger output of the intermittency circuit. These distributions, which of course peak at or near $\bar{Y}$, were also computer-fitted by polynominals. The microscale of the front is given by

$$\lambda_F = \frac{\sqrt{2}}{\pi} \frac{u(\bar{Y})}{N_o} \tag{10}$$

where $u(\bar{Y})$ is the jet velocity at $\bar{Y}$. An alternate, and possibly more meaningful front "wavelength" is simply

$$\Lambda_F \equiv \frac{u(\bar{Y})}{N_o} \tag{11}$$

3.1.2 RESULTS AND DISCUSSION

Figure 8 shows a typical comparison of the distributions, with radius, of the intermittency factor, the temperature, and the electron density. As expected, the fluid is strongly intermittent at distances from the axis at which the mean temperature is very close to the ambient. Also from Figure 8 it can be seen that the corresponding relation between electron density and the intermittency factor is analogous but highly inconsistent from one x to another: at a fixed value of $\gamma = 0.5$, for example, $\tilde{n}$ varies considerably in the x-range investigated.

Important questions to be settled in analyzing the intermittency data include the randomness of the interface, the coincidence between electron- and temperature-interface and the comparison of the front geometry and behavior to that of low-speed jets. The growth of the front "radius" $\bar{Y}$ is shown dimensionally in Figure 9 and non-dimensionally as $\bar{Y}/L$, together with the standard deviation σ/L, in Figure 10. There is little doubt that these two quantities grow linearly and scale with L, and that they certainly are independent of the method of measurement. With $\bar{Y}$ and σ so computed it is possible to make a test of the randomness of the front such as is shown on Figure 11; it is seen that the Gaussian distribution of the intermittency factor about the front position, that is with $(Y-\bar{Y})/\sigma$, again obtains in the fashion characteristic of stationary random variables. In the same figure further evidence of randomness is supplied by the distribution of the normalized crossing frequencies N/N_{max} about the radial location $Y_{max} = Y(N_{max})$. The scatter is appreciable, but enough data points are available to illustrate the Gaussian behavior of N/N_{max} characteristic of randomness. As before, there is no systematic difference between data taken with the hot-wire and data taken with the Langmuir probe.

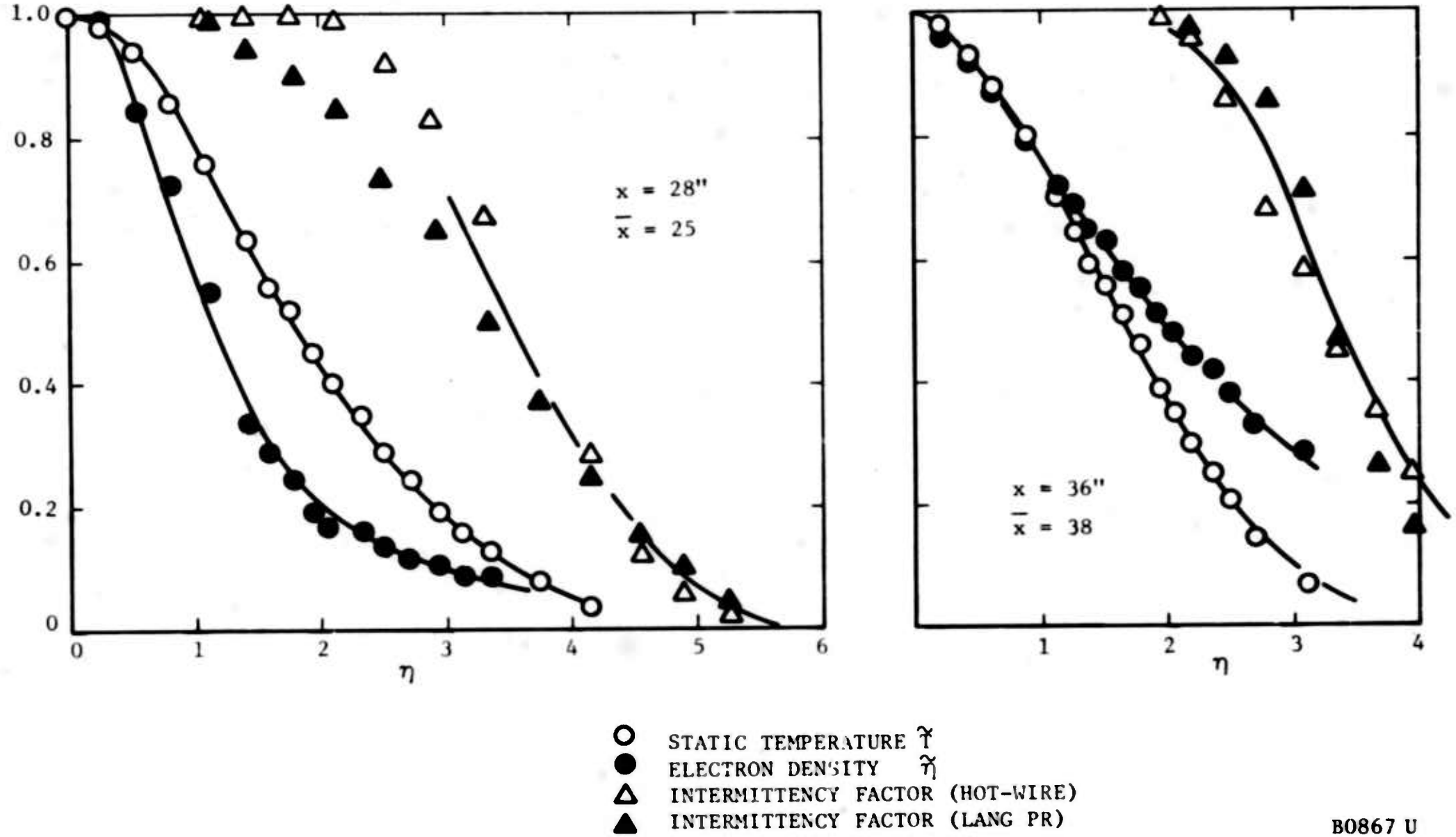

FIGURE 8 VARIATION OF INTERMITTENCY FACTOR IN THE JET, COMPARED WITH TYPICAL TEMPERATURES AND ELECTRON DENSITY DISTRIBUTIONS

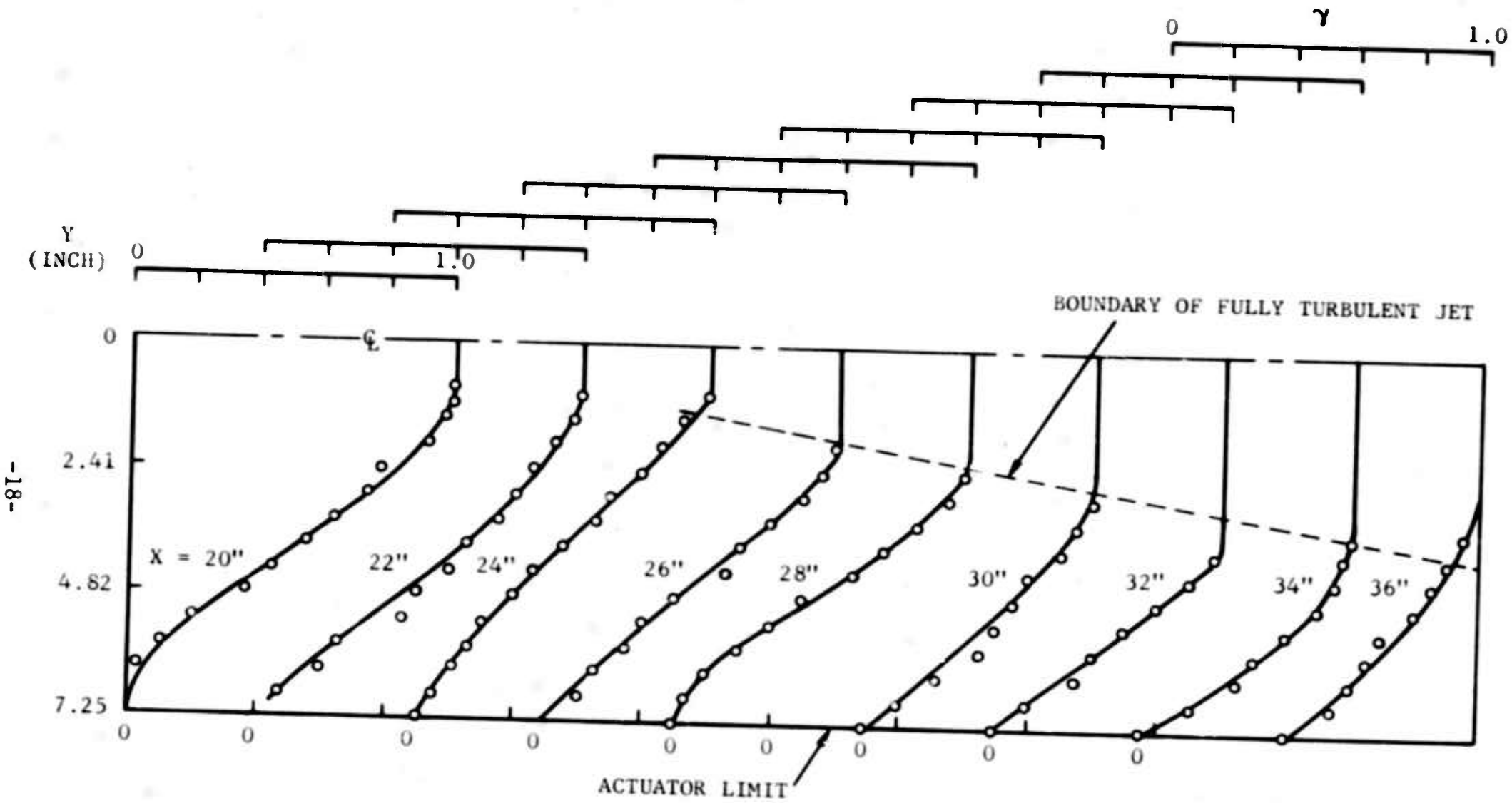

FIGURE 9 GROWTH OF THE BOUNDARY ENVELOPING THE FULLY TURBULENT JET FLUID

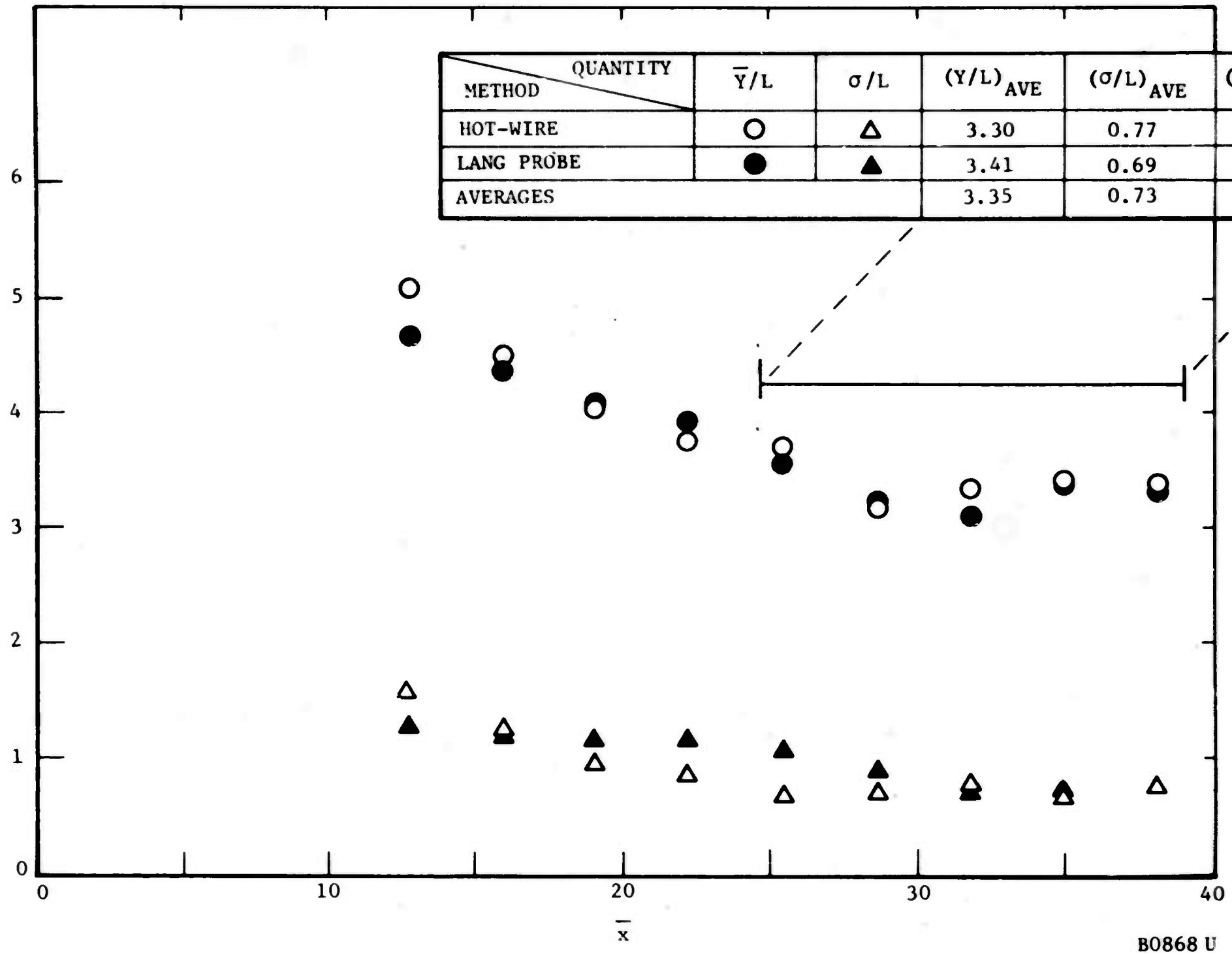

FIGURE 10 THE TURBULENT JET FRONT POSITION AND ITS STANDARD DEVIATION

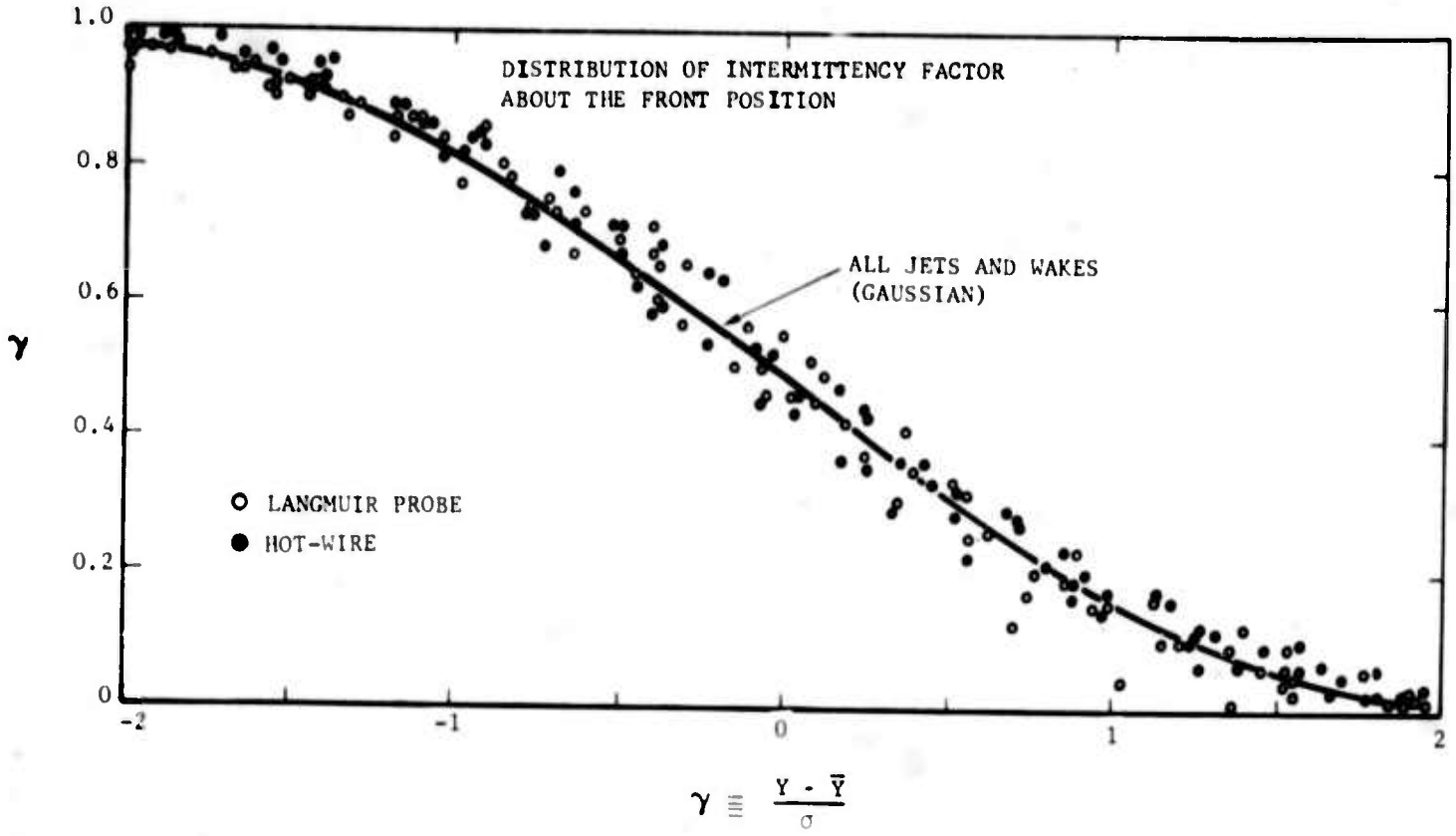

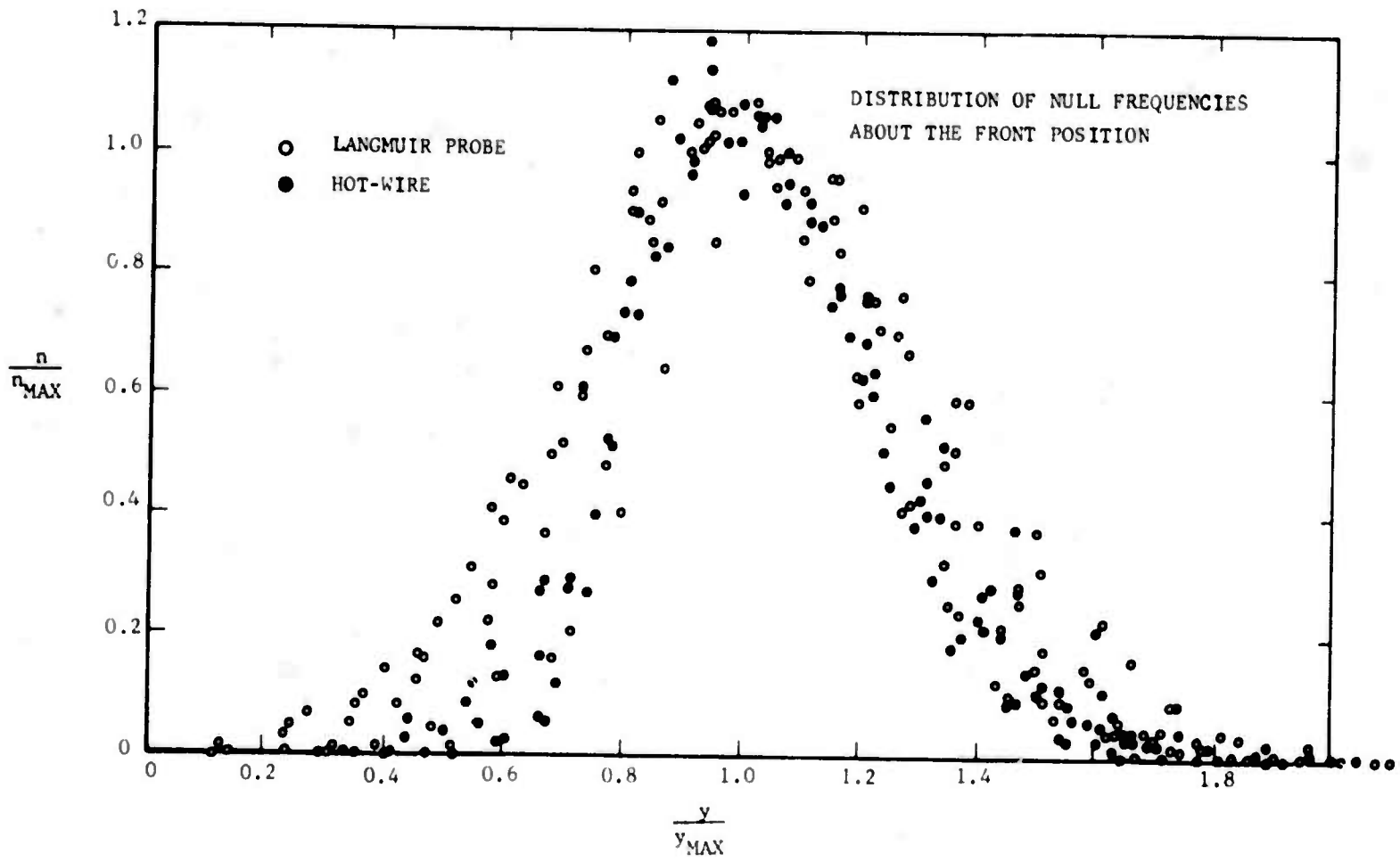

B0869U

FIGURE 11 DISTRIBUTION OF THE INTERMITTENCY FACTOR AND NULL-CROSSING FREQUENCIES ABOUT THE FRONT POSITION

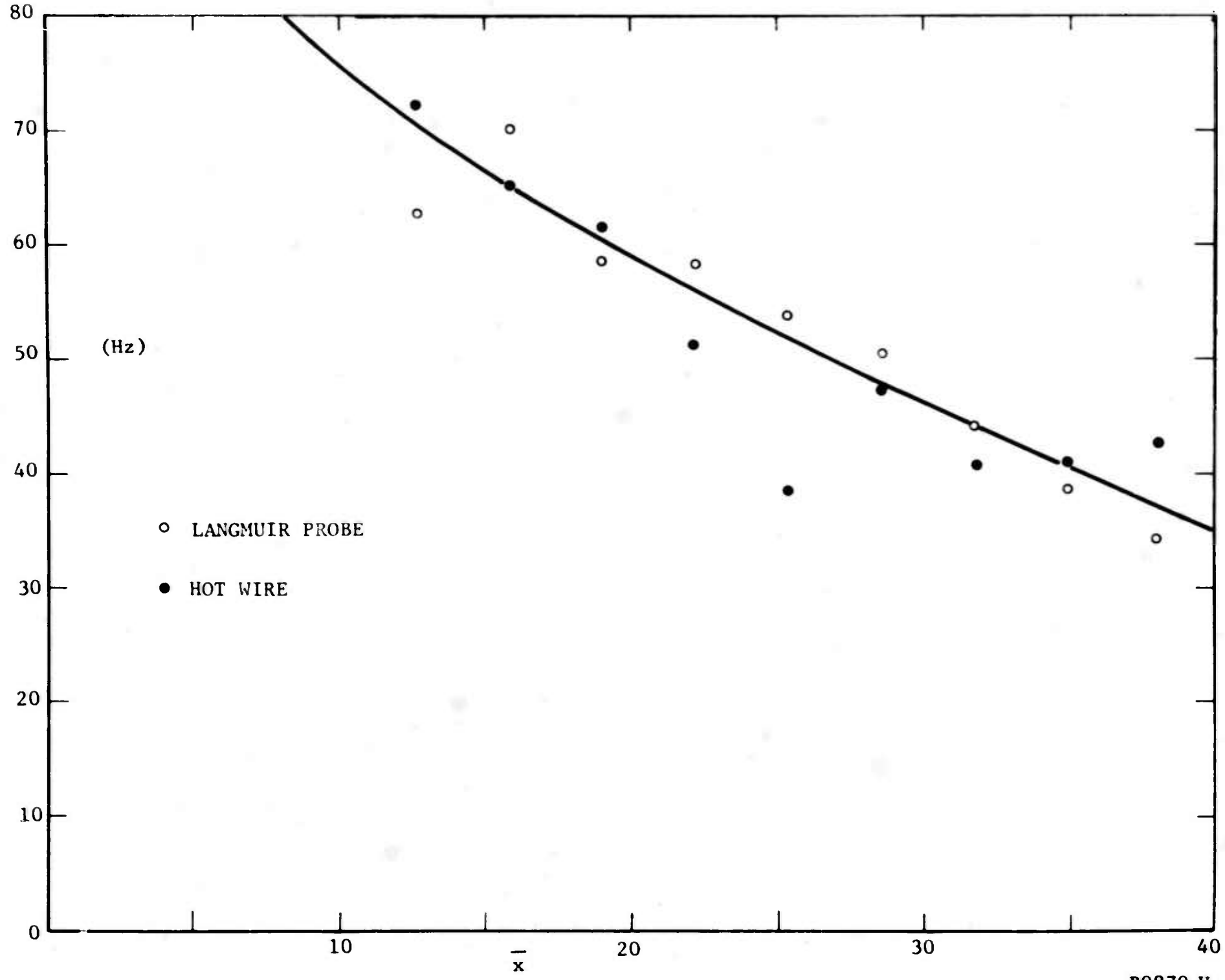

FIGURE 12 VARIATION OF THE NULL-CROSSING FREQUENCIES WITH DISTANCE

The null frequencies N_o, defined as the crossing frequencies measured at the position of the interface, were found to be very close to the maximum frequency N_{max} measured (at each x) at Y_{max} thus, $N_o \equiv N(Y_{max}) = N(\overline{Y}) = N_{max}$ as expected. Figure 12 shows the variation of N_o with x; again, the frequencies measured with the hot-wire and the Langmuir probe are about the same at each x. The decrease of N_o shown in this figure immediately suggests the lengthening of the front scale λ_F (or Λ_F) expected as the turbulent flow widens with distance. However, the computation of these scales from Equations (10) and (11) cannot be performed with the velocity data shown so far; these latter are mean velocities, whereas what is of course needed is the velocity of the front itself or at least the mean velocity within the front - the so-called eddy velocity.

Measurement of eddy velocities within "corrugations" in the jet boundary were made with the double Langmuir probe (two-wire correlation probe). Eddy velocities with such a probe can best be measured from the cross-correlation function of the probe signals; in the present work the more primitive method was adopted of obtaining a finite number of dual-trace oscillograms of the turbulence pattern as it was convected by the wires. From these samples a rudimentary statistical distribution of the local eddy velocity was constructed at each point from which the mean velocity (and its fluctuation) could be extracted. The (mean) eddy velocity at $\overline{Y}$ was then used in place of u in Equations (10) and (11).

Reference 5 describes experiments done on the intermittency features of compressible wakes and advises the use of the "front wavelength" Λ_F (rather than λ_F) as a more significant measure of the front geometry. In doing so, evidence is drawn from observations of the turbulence spectra (near the front position $\overline{Y}$) that the front itself may not be truly random, but rather weakly periodic at a wavelength Λ_F. The asymptotic from $\Lambda_F/L = u/N\ L$ of this wavelength for the axi-symmetric wake is drawn in Figure 13 in which the jet front wavelength, obtained per the previous paragraph, are also presented. The agreement between these two independent experiments is quite revealing. The wavelength of the jet front appears to bear the same relation to L (about $_F/L \simeq 9$) that it does for the wake.

It should be noted that the physical dimensions of the front are given here in physical coordinates, and this should be accounted for comparing the present results with other experiments. In the latter the radius is usually normalized with the so-called half-radius $r_{1/2}$. Thus Becker et.al (Reference 7) gives $\overline{Y}/r_{1/2} = 1.78$, Bradbury (Reference 8) 1.73 and Corrsin and Kistler (Reference 9) values ranging from 1.65 to 2.00. From the present experiment (see Figure 8) we obtain $\overline{Y}/L = 3.35$ on the average, and in terms of the half-radius we get $\overline{Y}/r_{1/2} = 2.0$ It therefore appears that quite a few jet experiments generally agree as to $\overline{Y}/r_{1/2}$. It should be remembered, however, that heating the fluid generally increases the jet radius; the end result, shown on Figure 14, is that our $\overline{Y}$ extends farther out, by about 30 percent, than Corrsin's $\overline{Y}$ for example.

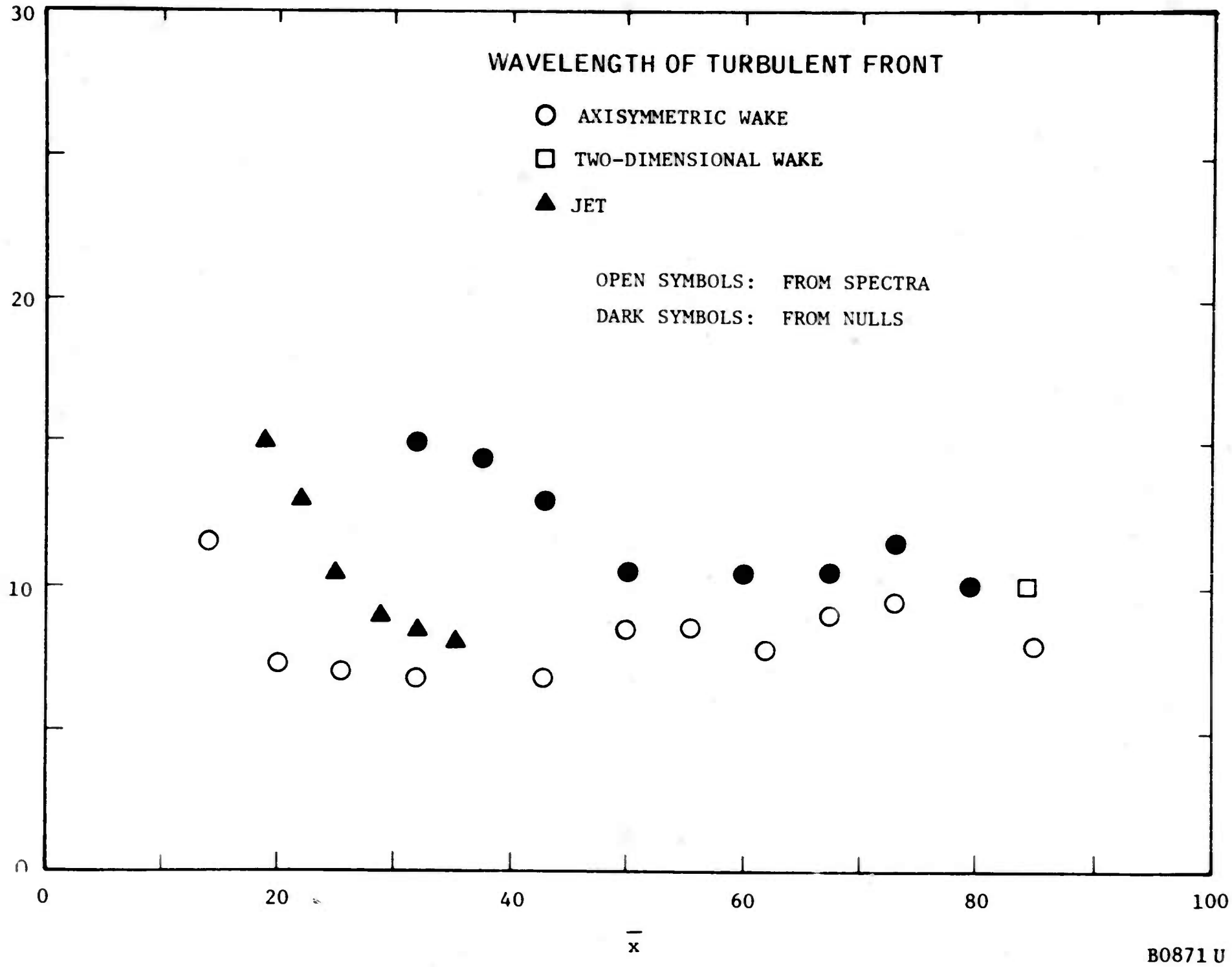

FIGURE 13 VARIATION OF FRONT WAVELENGTH OF TYPICAL FREE TURBULENT FLOWS

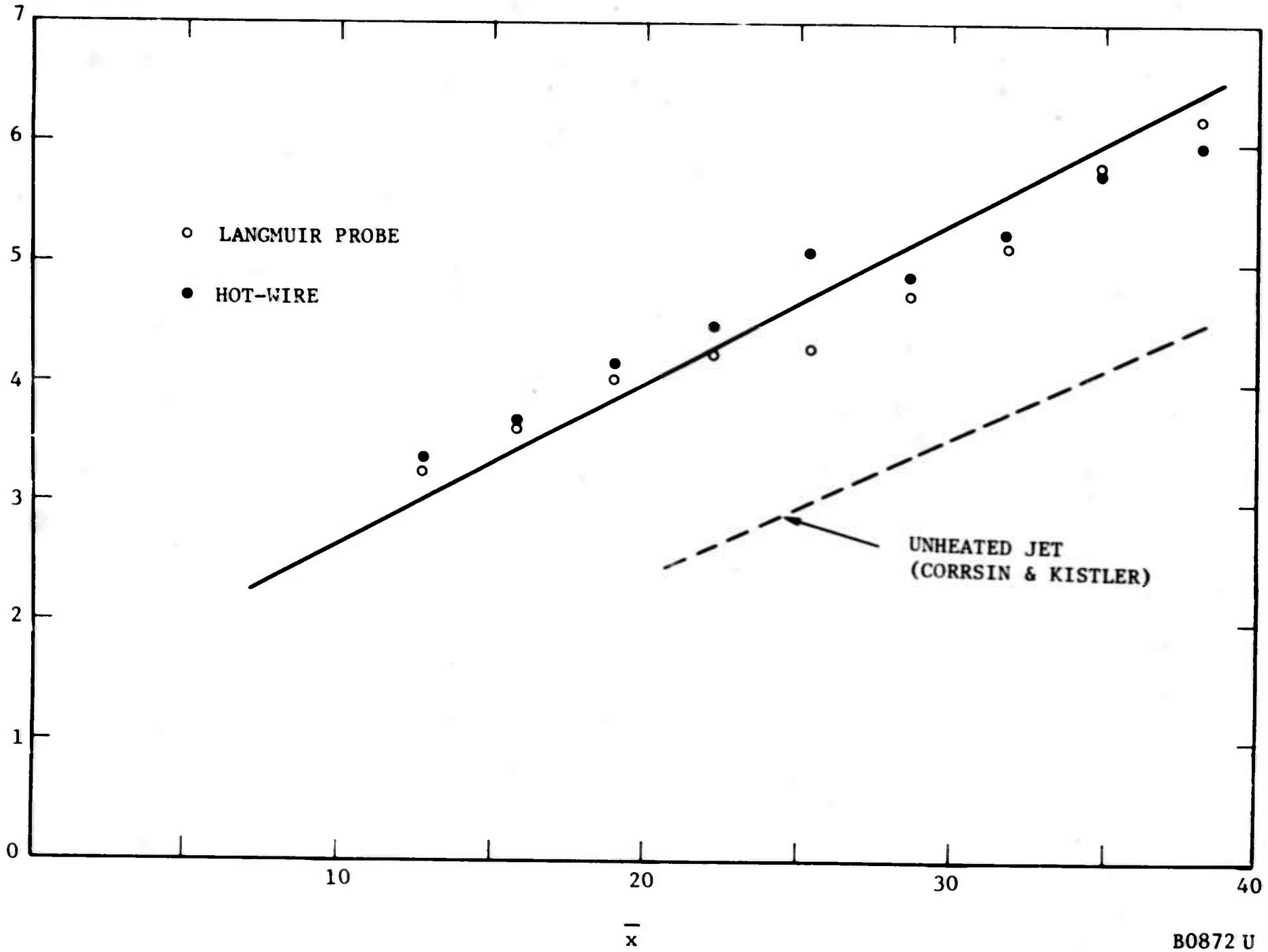

FIGURE 14 COMPARISON OF TURBULENT FRONT GROWTH WITH TYPICAL LOW-SPEED DATA

The value of σ/Y obtained here is 0.23, not far from Bradbury's value of 0.22 or Corrsin's range of 0.23 to 0.29. However Becker et.al. obtained $\sigma/Y = 0.16$. This might be interpreted as a difference in intermittent properties between an inert contaminant and the temperature field, but it is more likely that Becker's method of measurement and perhaps differences in the turbulent Reynolds number are responsible. Becker and his co-workers have at any rate obtained a unique relation between the intermittency factor and the contaminant density distribution with radius. In the reacting jet employed here the electrons are distributed radially in an irregular manner because of reactions (see Figure 8) and this relation does not materialize.

3.2 THE LARGE ELECTRON DENSITY FLUCTUATIONS

Perhaps the single most interesting phenomenon observed during the turbulence measurements was the very large magnitudes of the electron density fluctuation. It is statistically possible for the standard deviation of a stationary variable to exceed the mean value of the variable when the amplitude distribution of the latter is extremely skew. Such situations exist in the intermittent zones of ordinary turbulent jets for any flow variable Q which fluctuates between nil in the ambient ("irrotational") environment and some mean level within the turbulent front. If the latter does not decrease too fast with increasing radius then it is well known that $\Delta Q/Q$ can diverge with radial distance. In fact Becker, Hottel and Williams (Reference 7) have observed this divergence by utilizing an inert contaminant concentration for an observable.

The possibility that the large fluctuations on the axis pictured on Figure 15 are caused by the intermittency is excluded by the simple fact that the flow on the axis is fully turbulent as already demonstrated. From the results thus far shown in fact, it appears that we have here a fully turbulent fluid with normal temperature fluctuation but with highly-skewed electron fluctuations. An oscilloscopic study of the turbulent jet immediately showed large "spikes" in the electron density time history at a point; these spikes are indeed what statistics would require to produce the large $\Delta n/n$ of Figure 15. Figure 16 shows a comparative oscilloscope study of the Langmuir probe and hot-wire output at various radial positions but at the same distance from the jet nozzle. By properly adjusting the scope gain it is possible to show conclusively, first, the differences between intermittent and fully turbulent flow and, secondly, the differences between Langmuir-probe and hot-wire output in the fully turbulent region. Attention is drawn to the large spikes in the Langmuir probe traces which are clearly absent from the hot-wire traces.

The appearance of the large spikes persisted for several inches in the upstream end of the turbulent zone studied, but decayed and eventually vanished as the probe was moved downstream; the fluctuation level $\Delta n/n$ also decayed below unity as Figure 15 shows. To complete the picture, an investigation of the laminar and transitional portions of the jet was made

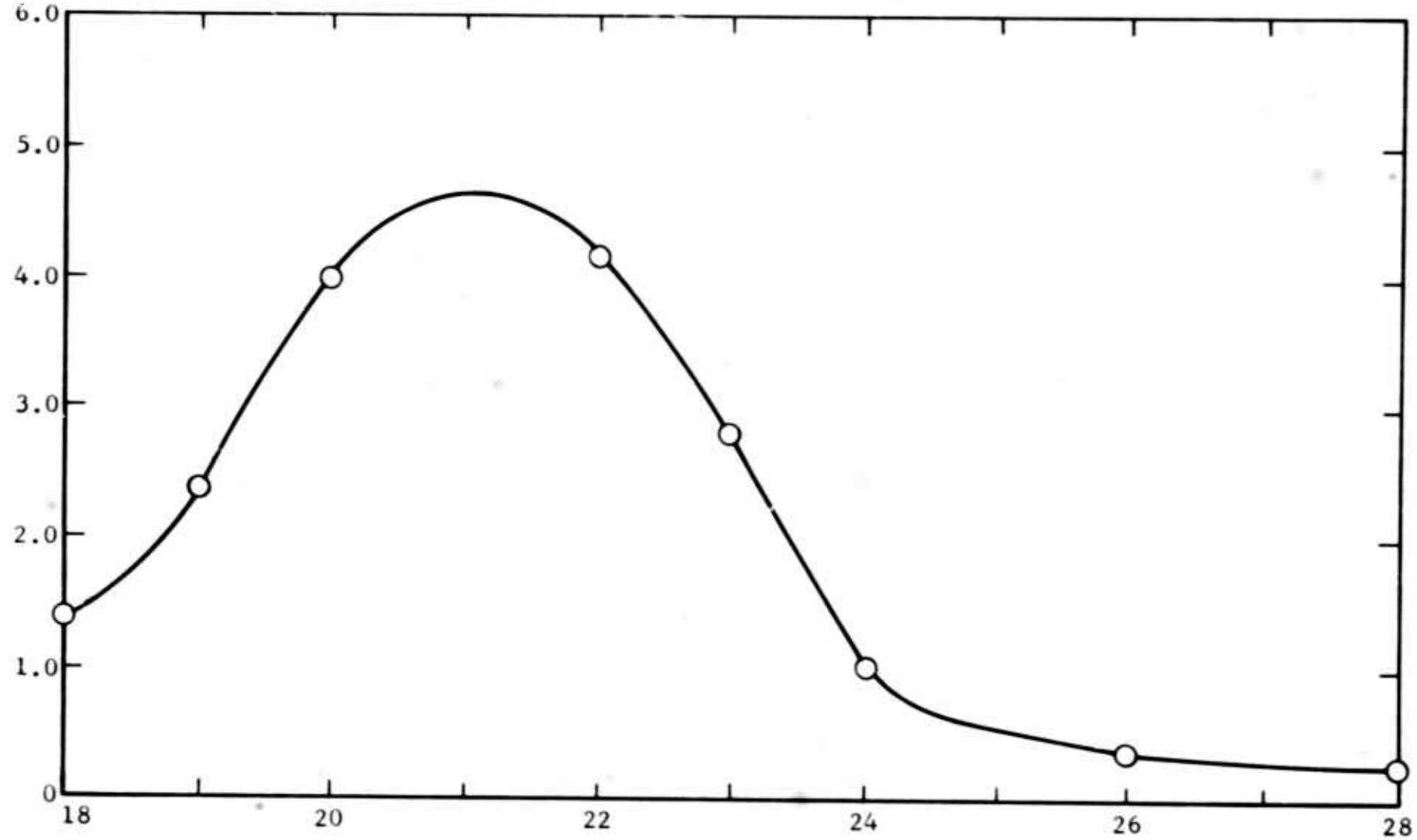

F12177 U

FIGURE 15 VARIATION OF NORMALIZED ELECTRON DENSITY FLUCTUATIONS ALONG THE JET AXIS

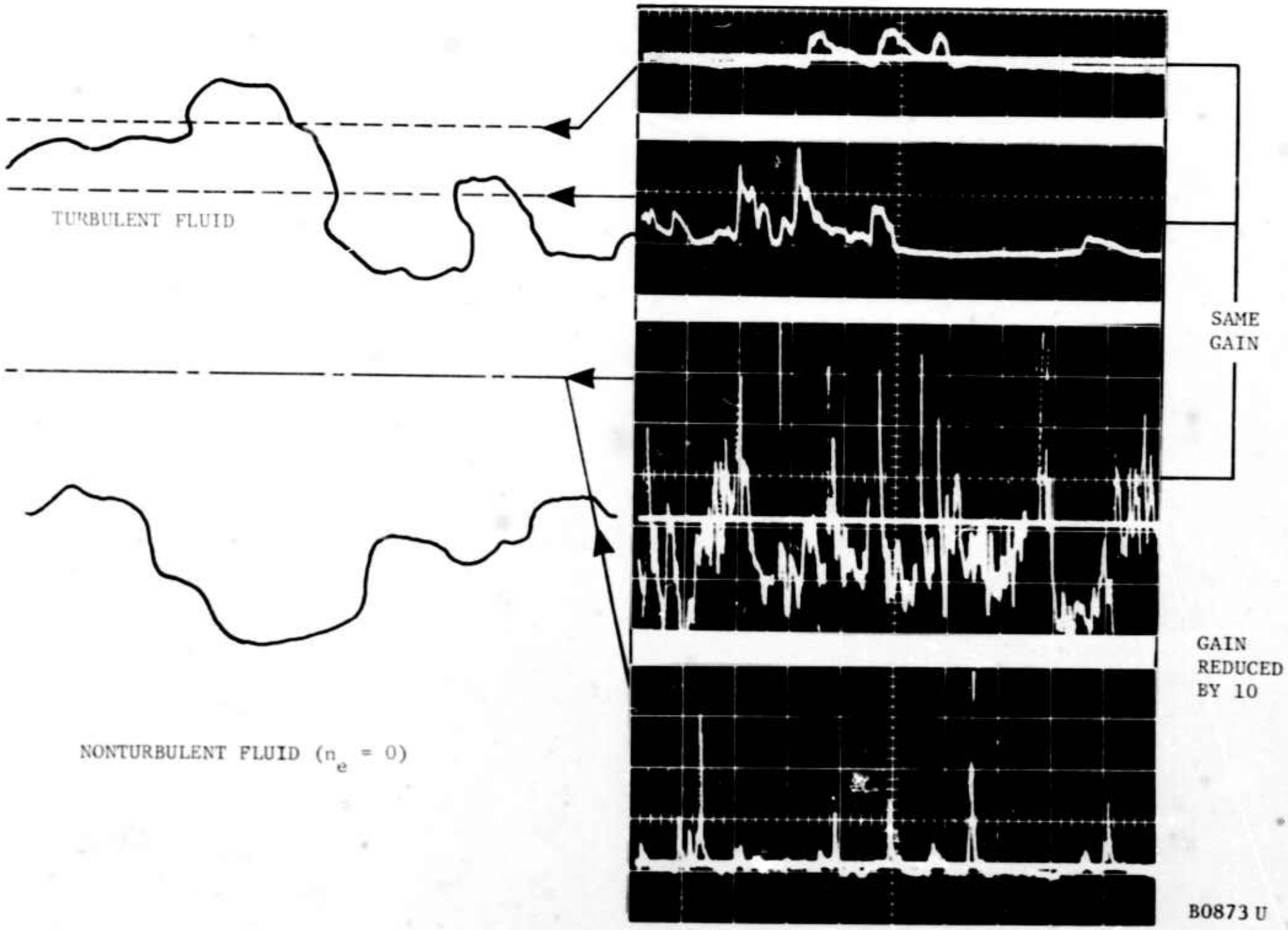

FIGURE 16 OSCILLOSCOPIC STUDY OF TEMPERATURE AND ELECTRON DENSITY FLUCTUATIONS (1 OF 2)

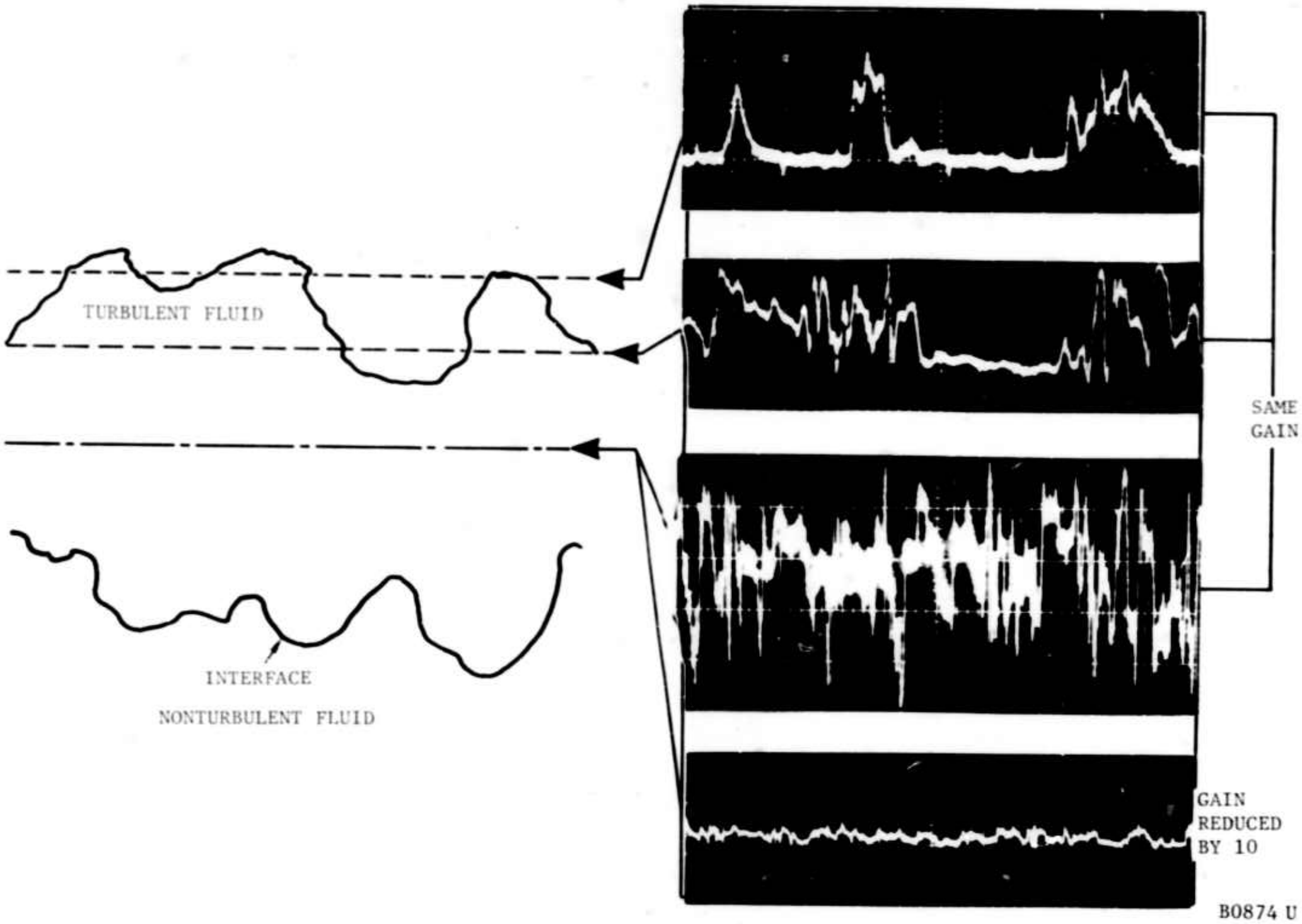

FIGURE 16 OSCILLOSCOPE STUDY OF TEMPERATURE AND ELECTRON DENSITY FLUCTUATIONS (2 OF 2)

using a Langmuir probe thicker than described previously in this paper, so that it could withstand the much higher heat fluxes in the laminar jet. For obvious reasons the output of this probe was not quantitatively interpretable, but it made possible to piece together a reasonable description of the events leading to the generation of the large fluctuations.

Figure 17 shows this picture. The Langmuir probe observation made is typified by an instantaneous "snapshot" of the electron density on the jet axis from the nozzle exit well into the turbulent zone. In the laminar jet the mean electron density is high with an unsteady component consisting of the rectifier-driven 360 HZ modulation whose rms magnitude is about 10 percent of the mean. At the flow velocities prevalent here the wavelength of this sinusoidal fluctuation is actually very much larger than the length of the laminar jet (about 10 feet compared to about 1 foot). In the transition region the breakdown process mixes ambient fluid with the ionized fluid; the former is electron-poor so that large "negative" pulses (if one thinks of the electron current as producing a positive displacement of the scope beam) appear as shown on Figure 17: the signal is thus "negatively one-sided". The mean electron density thus decreases below the maximum level - which also decreases because of recombinations. Farther downstream the spikes widen (but do not necessarily deepen), and still farther the signal begins reversing itself, i.e., becoming "positively one-sided". In this latter case the mean electron density drops considerably below the tops of the spikes, the fluctuation distribution is very skew and the rms fluctuation level is considerably higher than the mean level. It is at this stage that the oscillograms shown on Figure 16 were taken.

It should be again emphasized that at this stage the fluid is fully turbulent from the standpoint of intermittency, and that turbulent fluctuations in the electron density, of order 20 to 40 percent of the mean, exist in addition to the large electron density spikes. The latter are obviously the remnants of the laminar flow upstream of the transition zone, in which the electron density level is very high when compared to the level in the turbulent fluid itself. Eventually these spikes also disappear and, as Figure 15 shows, the ratio $\Delta n/n$ settles to values of order 20 percent in the far jet.

In Figure 17 it is schematically shown that the maximum of the normalized fluctuations is attained where the mean electron level is much below the maximum level n_m, that is the locus of the spike maxima. If the spikes are truly the results of the process of engulfment of the ambient, electron-poor fluid by the electron-rich fluid of the jet, and if the electron density of the former is n_c, then

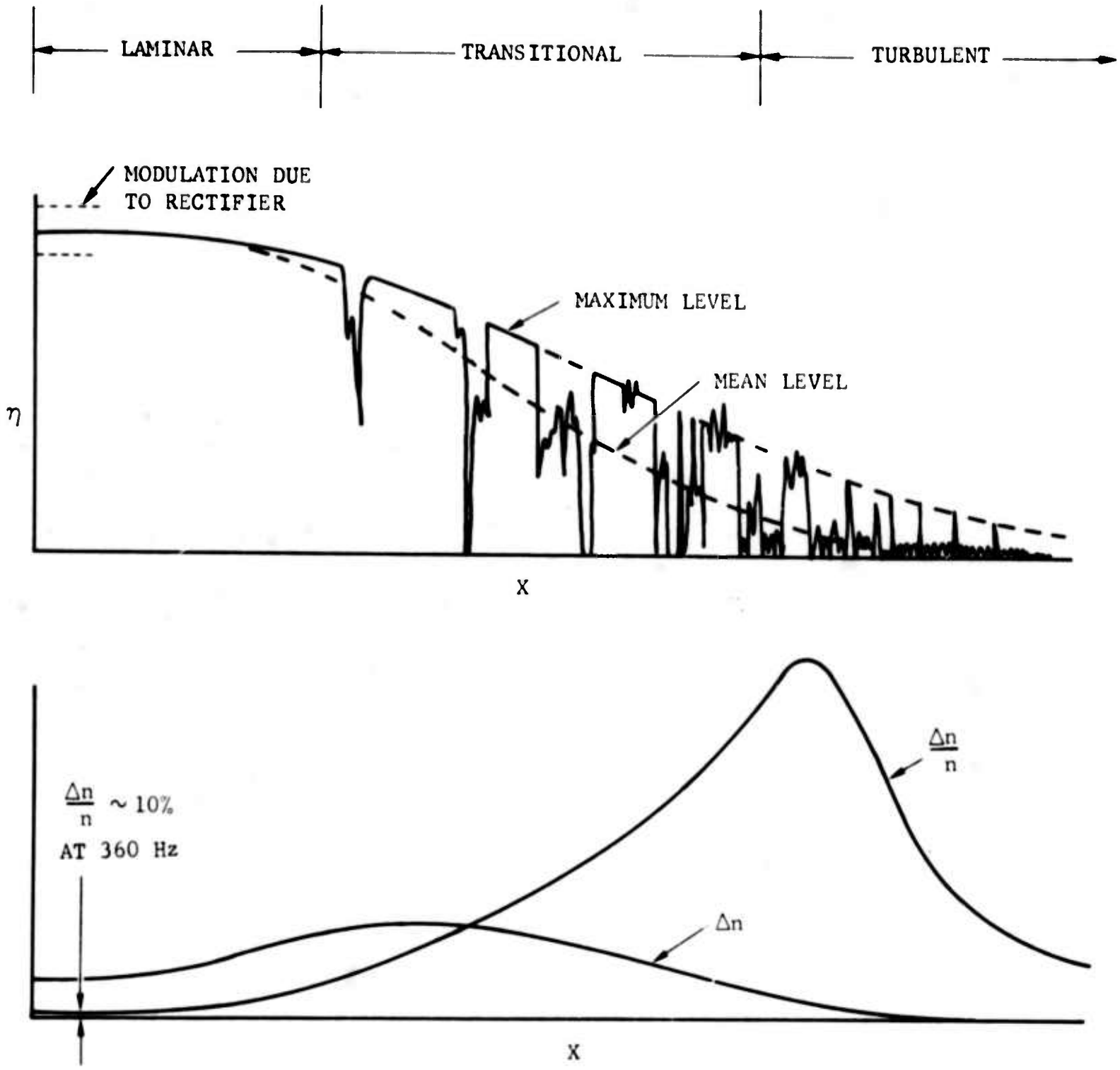

FIGURE 17 RECONSTRUCTED "SNAPSHOT" OF THE DISTRIBUTION OF ELECTRON DENSITY ALONG THE JET

$$\left(\frac{\Delta \bar{n}}{n}\right)^2 (x) = \frac{(n_m/n_c - 1)^2 (P/\dot{m} - 1)}{(n_m/n_c - 1) + P/\dot{m}^2} \qquad (12)$$

where $P/\dot{m}$ is the ratio of the total mass to the jet mass. Here it has been assumed that both fluid components are laminar so that the signal can locally oscillate between n_m and n_c only, in the manner suggested some time ago by Feldman and Proudian (Reference 10) and Lin (Reference 11). The type of fluctuations of Equation (12) are nil before entrainment begins ($P/\dot{m} = 1$) and also when $P/\dot{m}$ tends to infinity in the far jet, and they peak in between with a magnitude depending on n_m/n_c. For equilibrium chemistry, where n_m and n_c are directly obtainable from the corresponding temperature T_m and T_c, it is shown by Reference 12 that $\Delta n/n$ of order 10^6 or higher can obtain for practical values of T_m/T_c. For finite reaction rates the ratio $\Delta n/n$ becomes extremely sensitive to the chemistry.

Nevertheless the simplicity of the jet flow brought about by gas-dynamical self-preservation allows certain broad tests of Equation (12) to be made easily. For example the entrainment rate is given theoretically and has alsc been measured directly. For recombination reactions the n_m might also be obtained as a function of x. The normalized electron density fluctuations of Equation (12) thus become dependent only on the ratio n_{m_o} (of the maximum electron density in the laminar flow) to the"ambient" value n_c. The former is actually obtainable from the experiment but the latter is not, since the electron density at the base of the spikes was detected to be turbulent and of a mean value much higher than that outside the jet. Computations made with Equation (12) using estimated values of n_c gave reasonable numerical agreement with the measured axial variation of $\Delta n/n$ shown on Figure 15.

Equation (12) thus appears to be a reasonable descriptor of the physical mechanism giving rise to the large electron density fluctuations - on the strength of the mixing model it describes. It does not necessarily endorse the "laminar mixing" ideas of References 10 and 11 since the participating lumps of fluid (whether electron-rich or electron-poor) are turbulent in character. At this time it also appears to affect the transitional zone more so than the turbulent activity in the far jet; in the present experiment thus zone is only a few jet thicknesses long.

SECTION IV

SUPERSONIC WAKES AT ANGLE OF ATTACK

4.1 INTRODUCTION

Drastic changes are introduced in the wake of a body flying at supersonic speeds when the body is inclined at some incidence (angle of attack) with respect to the flight vector: first, the increased total drag generates an intense inviscid wake, i.e., large gradients appear in the flow surrounding the inner, or turbulent wake. Secondly, these gradients are generally asymmetric about the wake axis. Thirdly, changes in the viscous drag change the characteristics of the viscous wake. Finally, with the generation of lifting forces vortical flows migh also appear, causing added complexities to the flow field.

Although the new character of the turbulent wake is hard to assess in these circumstances, its role in the mixing process can be predicted along general lines. Its main complexity should be its growth in and interaction with the asymmetric inviscid wake. The flow thus consists of a "shear layer" contributed to by the inviscid wake, with a superposed wake flow. It is quite clear that the behavior of this composite flow cannot always follow simple wake rules of lateral growth, for example, or of velocity decay, since shear layers and wakes are generally governed by different rules. Thus, a pure shear layer supplies a constant reference velocity scale by definition, while the corresponding velocity scale of the wake decreases with distance. In limiting cases, the competition between the shear-layer-like and wake-like behavior can be foreseen: for small angles of attack and large shear drag, the wake-like behavior should dominate early, while for inclination angles large enough to cause very persistent inviscid asymmetries the flow is probably shear-layer-like for large distances.

The present experiment was designed mainly in a way so as to accentuate this competition between the inviscid and the viscous (turbulent) wake. Calculations of the supersonic inviscid flow behind a two-dimensional slender body at incidence, verified experimentally, showed a considerable persistence of asymmetries in a pattern approaching an ideal shear layer. Thus, the problem is not only relevant, but was done in a way capable of fundamental conclusions on the basic behavior of fluids.

4.2 MODEL AND FACILITIES

This work is performed in the Philco-Ford supersonic wind-tunnel at a continuous air flow at Mach 3.0, a stagnation pressure of 730 mm Hg absolute and a total temperature of 39°C; the tunnel is described in detail in Reference 13. The model consisted of a 0.004-inch thick, 0.116-inch wide stainless-steel ribbon stretched across the tunnel test-section, identical to that used in the WED experiment (two-dimensional adiabatic wake at zero incidence) and described in detail in Reference 1. A major modification to the model support consisted of the addition of a fixed steel protractor and

pointer by which incidence angle could be set and resolved to better than 0.25 degree twist-angle resolution is about 0.1 degree. Other modifications to the support, described in Section V were made to accomodate the heat-transfer experiment. The protractor is shown on Figure 18. Figure 19 shows the arrangement of the model and the nomenclature of the flow phenomena and coordinate axes.

4.3 EXPERIMENT DESIGN

4.3.1 INVISCID WAKE

Detailed calculations of the inviscid wake of the flat plate were made using the method of two-dimensional characteristics at an angle of attack of 20 degrees; for different angles, the flow field should not alter greatly from this calculation, provided that the incidence angle for shock detachment at the leading edge (about 34 degrees at this Mach number) is not exceeded. In this calculation the upstream boundary conditions on the windward side were the oblique shock at the leading edge; for the leeward side, the trailing edge shock as modified by the leading-edge expansion fan. Figure 20 shows graphically the results. Attention should be drawn to the two nearly parallel streamlines showning on either side of the wake axis. It turns out that these demark abruptly changing conditions in the sense of flow gradients (not in the sense of flow discontinuities). The net result is that between each of these two streamlines and the axis there appears a uniform "plateau" in flow conditions; the two adjacent "plateau" constitute, then, a shear-layer situation which apparently does not decay much, either in extent or intensity, as one moves downstream. Typical such plateaus are seen in cross-sectional views of Figure 20 shown in Figure 21.

The calculations outlined above demonstrate that, although quantitatively different for the axisymmetric hypersonic wake, an essential feature of the wake-at-incidence problem could indeed be obtained in our wind-tunnel. As described in the following paragraphs, the shear-layer feature was clearly evident from the data collected so far.

4.3.2 CHOICE OF INCIDENCE SETTINGS

To study the effect of incidence, more than one incidence angle should be chosen, if possible; a judicious choice of angles is needed in order to illuminate the effect without undue labor. It is known on theoretical grounds that beyond the detachment angle (34 degrees) the inviscid wake "freezes" to a configuration not very sensitive to angle of incidence. Tests verified this effect, and in the detached case it was decided to work only with $\alpha = 90°$ (plate normal to the stream) so that the blunt-body turbulent wake could at least be probed.

In the pre-detachment range of α wake "pitot maps", such as shown for $\alpha = 0°$ on Figure 30 of Reference 1, were taken at $\alpha = 10°$, $15°$, $20°$ and $30°$. Such maps are easy to construct and are invaluable in giving an overall picture of the flow field. Since the shear-layer-like behavior was present in each case, the angles $\alpha = 10°$ and $20°$ were chosen for further study.

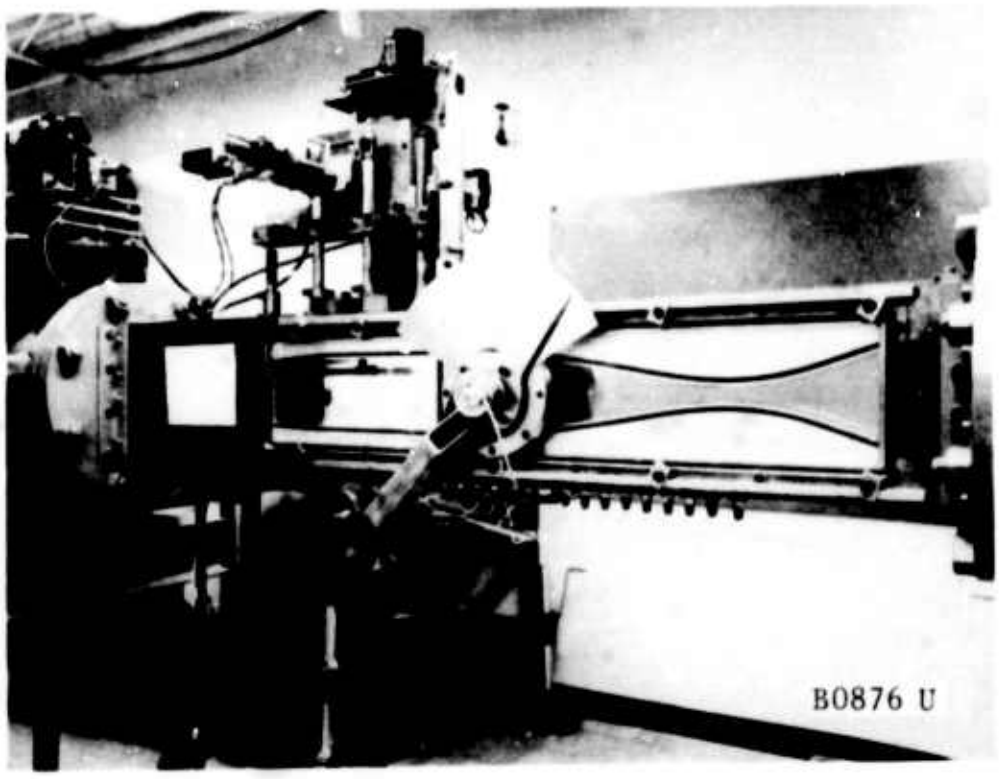

FIGURE 18 PHOTOGRAPH OF WIND-TUNNEL TEST-SECTION SHOWING TWO-DIMENSIONAL MODEL SUPPORT

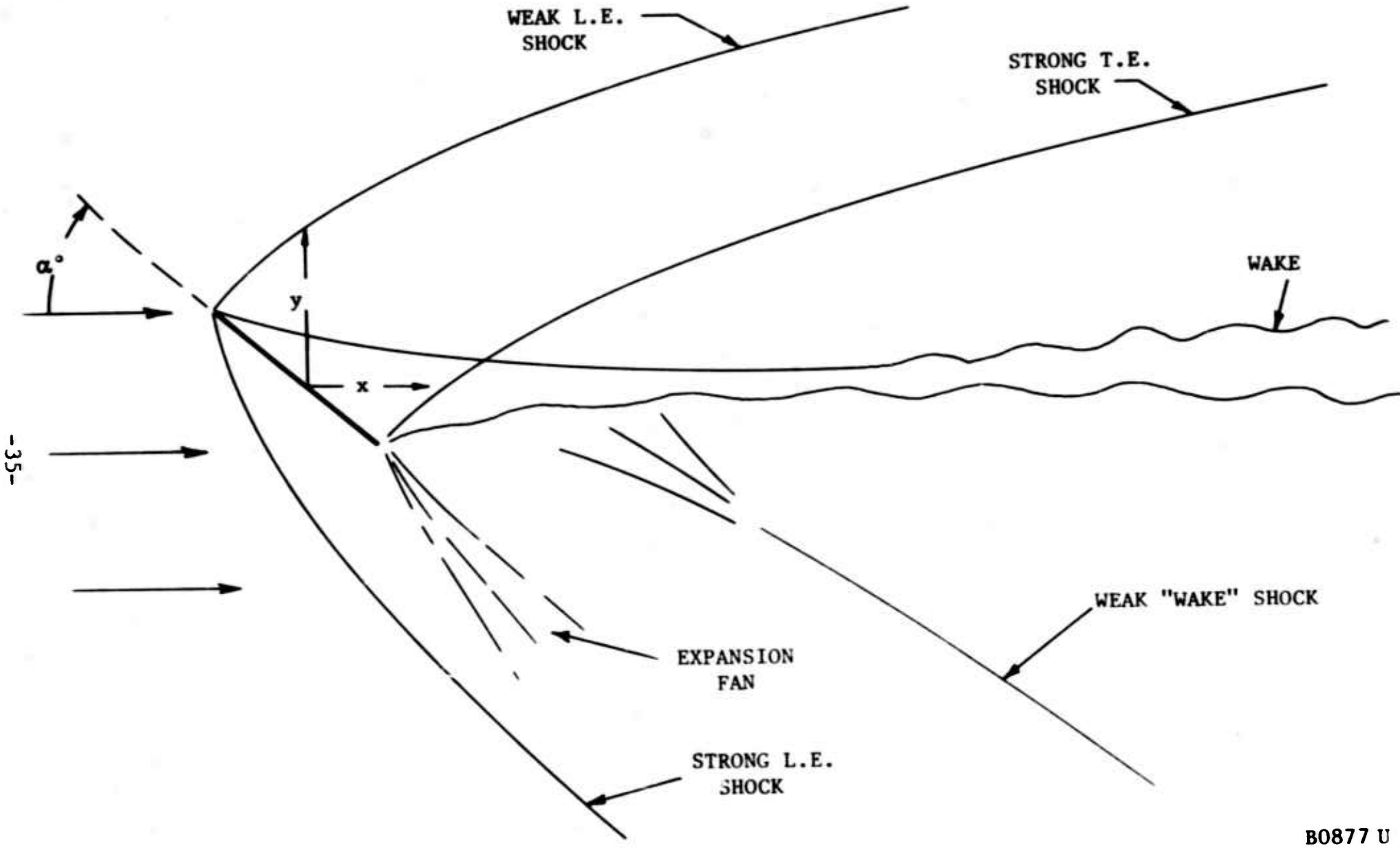

FIGURE 19 SCHEMATIC OF TWO-DIMENSIONAL WAKE NOMENCLATURE

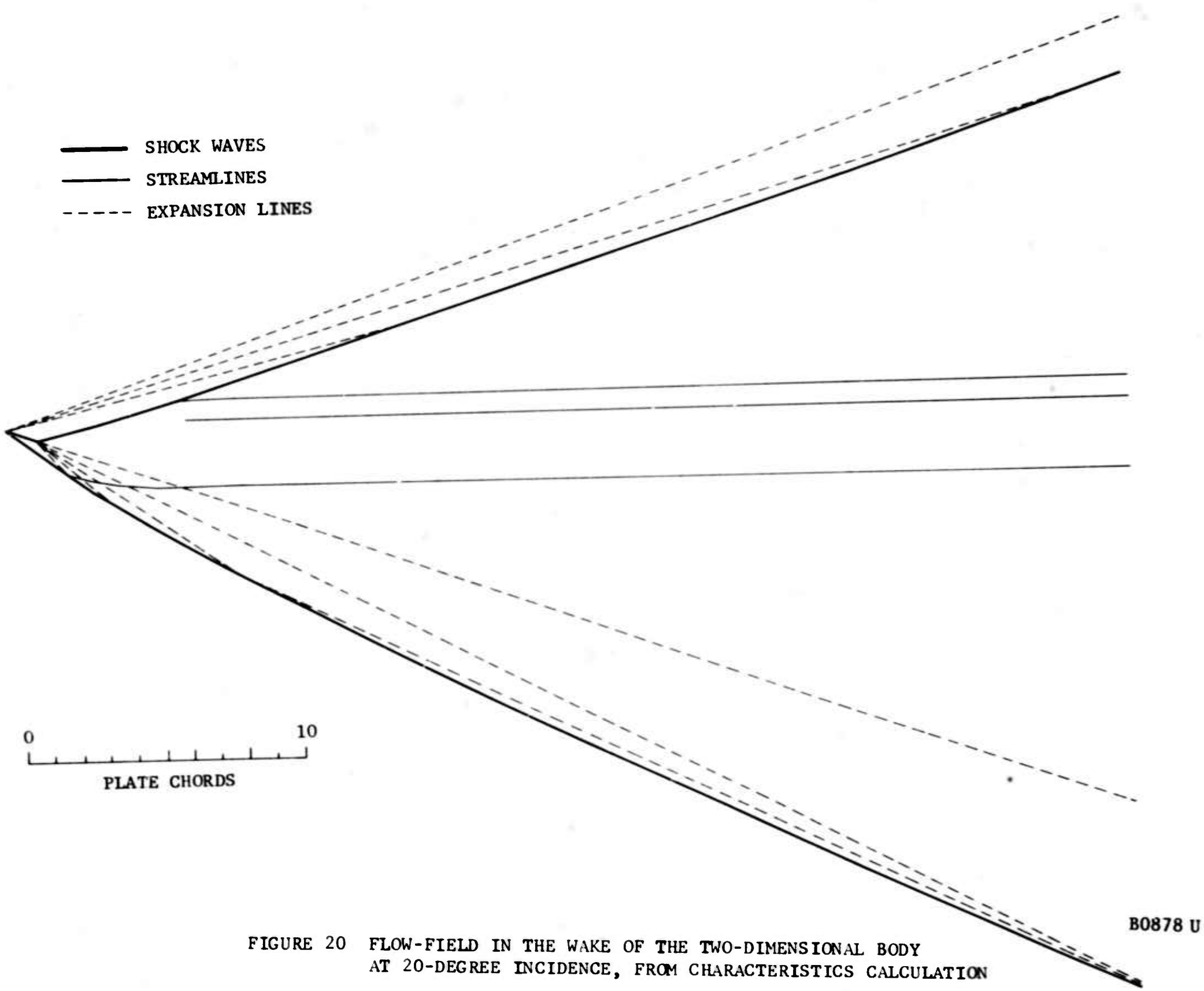

FIGURE 20 FLOW-FIELD IN THE WAKE OF THE TWO-DIMENSIONAL BODY AT 20-DEGREE INCIDENCE, FROM CHARACTERISTICS CALCULATION

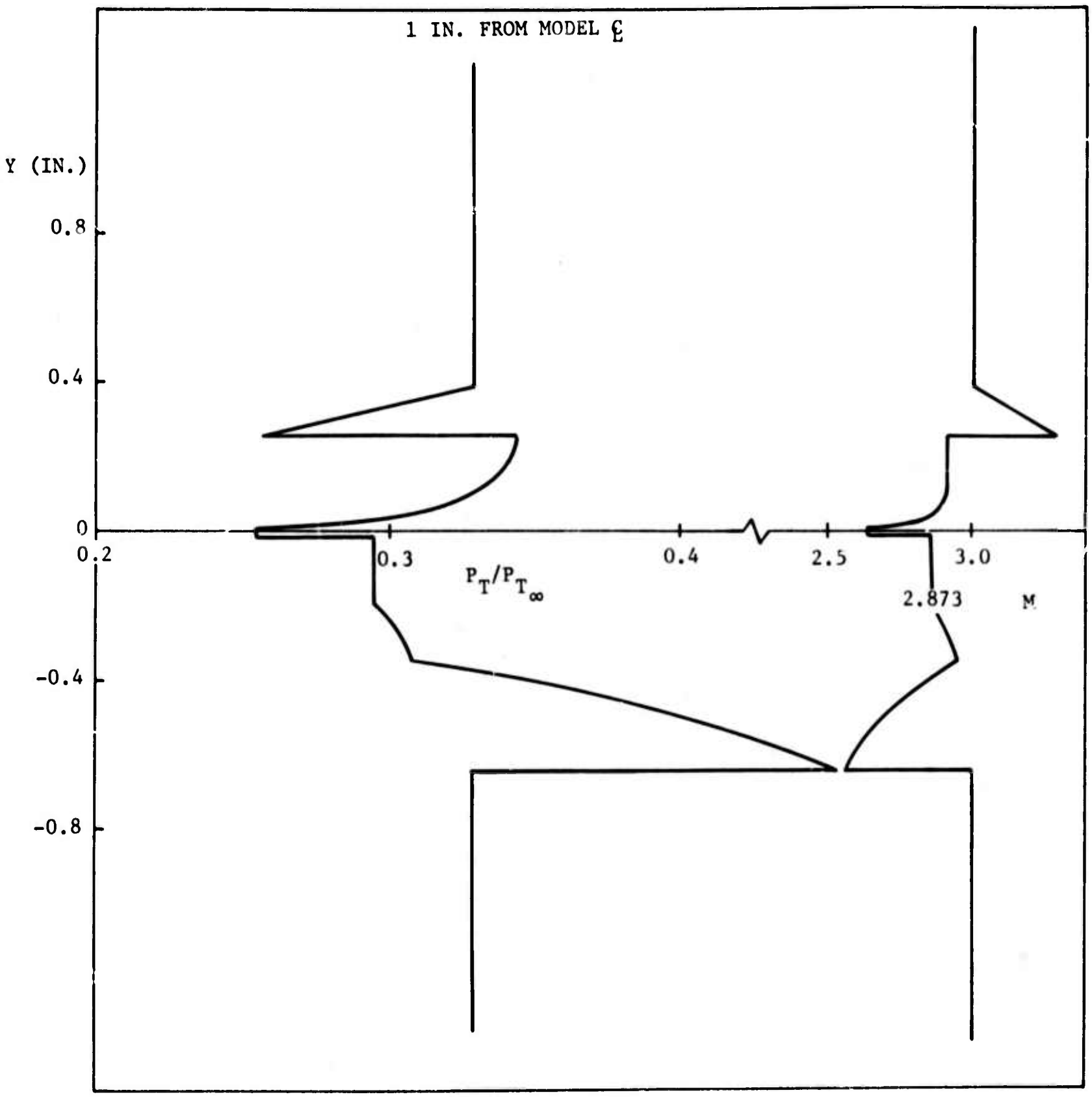
1 IN. FROM MODEL ℄
Y (IN.)
0.8
0.4
0
-0.4
-0.8
0.2
0.3
P_T/P_{T_∞}
0.4
2.5
3.0
2.873
M

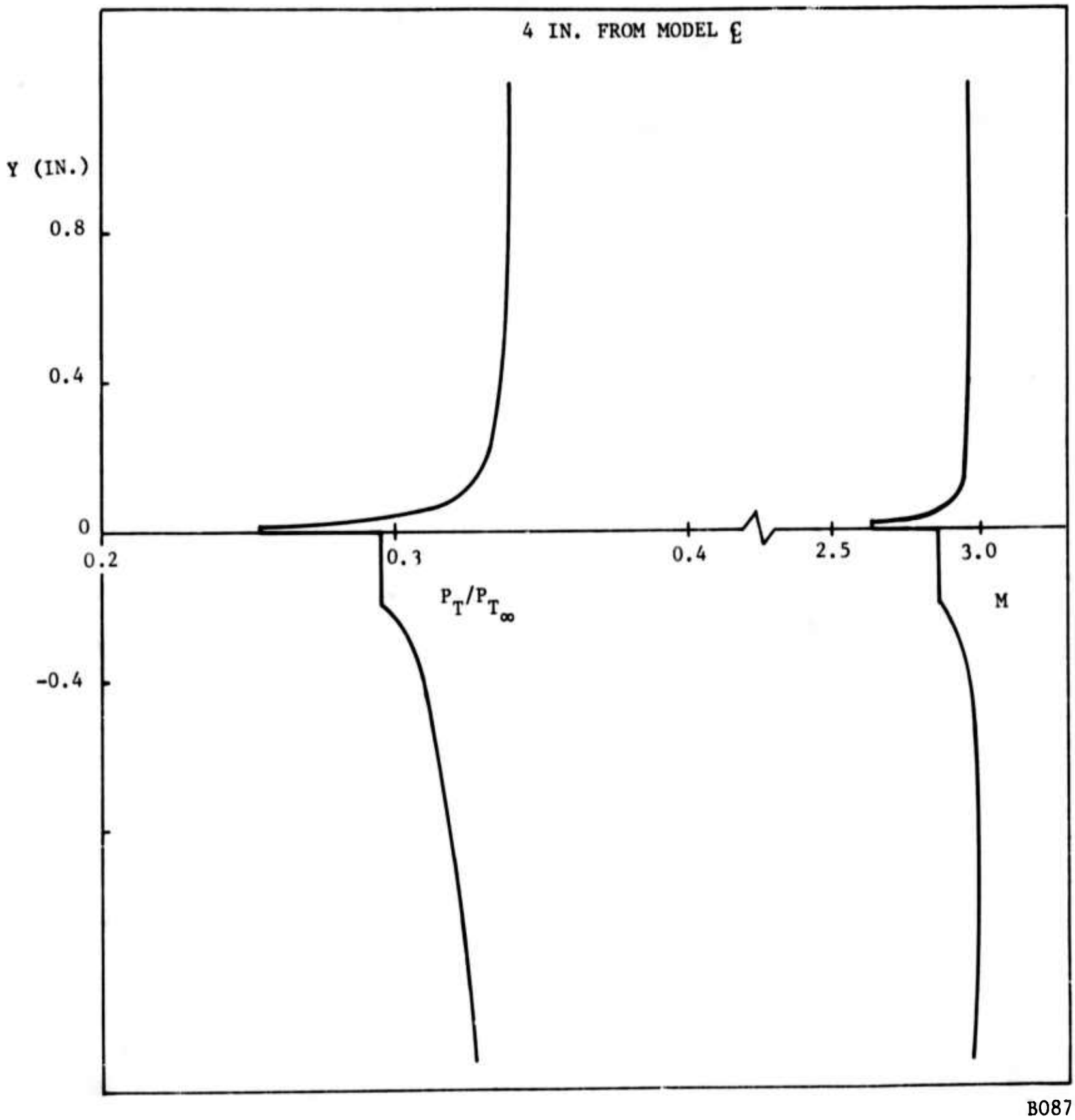

FIGURE 21 FLOW PROPERTIES AT FIXED DISTANCES BEHIND THE MODEL AT 20-DEGREE INCIDENCE

In designing the experiment, the farthest downstream distance where measurements can be made is important to know. In the wind-tunnel this distance is shortened when the model is pitched because of the earlier reflection of the strengthened shocks from the tunnel wall. In the present set-up the farthest downstream distance for α = 0°, 10°, 20° and 90° is 7.8 inches, 7 inches, 6.2 inches and 4.7 inches, respectively. Note that for α = 0°, a distance of 7.8 inches implies a distance of about 1,800 virtual body diameters.

4.4 DIAGNOSTIC INSTRUMENTATION

The diagnostic tools used for this experiment were identical to those employed for the WED (see Reference 1). The 0.00005 inch diameter Pt 10 percent Rh hot-wire used for this work managed to stay intact through the mean-flow and turbulence measurements and through most of the spectral measurements. This remarkable wire survived 45 calendar days of use, during which time it was operated for about 70 hours in supersonic flow. Through frequent oven- and flow-calibrations small changes in its characteristics could be monitored and accounted for.

4.5 PROCEDURE

This experiment was designated WEF (Wake Experiment F) and the α = 10°, 20°, and 90° sub-experiments were designated WEF-10, WEF-20, and WEF-90, respectively. As done with the WED experiment, the distance between the model mid-chord and the end (farthest downstream) point was marked by X-stations spaced by 0.300 inch increments. Continuous analog traverses were taken at each X station with the pitot and static probes and the hot-wire anemometer, the latter operated either in the mean-flow or the turbulent mode. From these data the mean and turbulent properties can be extracted.

4.6 RESULTS OF MEASUREMENTS

As already mentioned, the actual viscous wake measurements were preceded by tracing the inviscid wake in order to observe the overall flow field and to examine the existence of the "shear-layer" effect. Figure 22 compares a typical pitot traverse with the pitot pressure expected from the characteristics computation shown on Figures 20 and 21 for α = 20°. It is obvious from the measurement that two shocks appear on each side of the inviscid wake, instead of one as given by the characteristics method. On the windward side, and in addition to the bow shock at the leading edge, a second shock is thought to originate in the recompression region of the wake "neck", as illustrated tentatively on Figure 19. In the leeward side a shock appears, of course, at the model leading edge in addition to the expansion fan.*

*Photography of the two-dimensional model itself is impossible because of obstructions. The identification of the additional two shocks is left to reasonable conjecture.

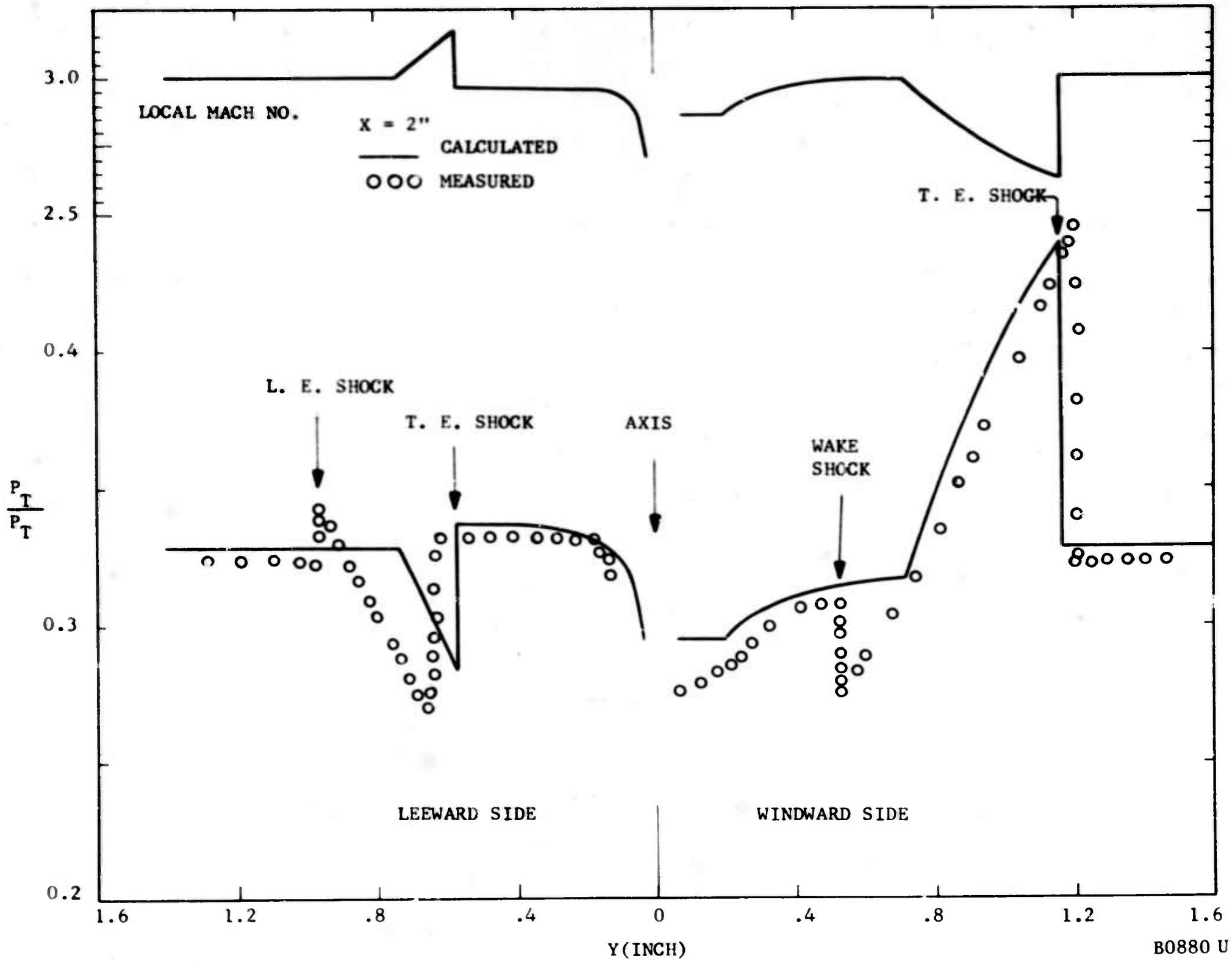

FIGURE 22 THEORETICAL AND EXPERIMENTAL DEDUCTION OF FLOW PROPERTIES IN THE WAKE

Nevertheless the agreement shown on Figure 21 between the calculated and measured pitot pressures is adequate; both demonstrate, in fact, the "plateaus" on either side of the turbulent wake.

A second preliminary measurement made before detailed studies were attempted concerned the existence of turbulence. Qualitative traverses with the hot-wire showed that angle of attack did not inhibit the appearance of turbulence in the inner wake. Proceeding to the latter, Figure 23 shows pitot-pressure traces at typical X stations for all three experiments, i.e., WEF-10, WEF-20, and WEF-90. A trace for WED (corresponding to WEF-0) is also shown. The object of this figure is to demonstrate the wake symmetry which understandably obtains for the symmetric body configurations, namely for WED and WEF-90. Note, also, the expected change in "free-stream" pitot level for the WEF-10 and WEF-20 traces, illustrating the "shear-layer" effect.

Typical static pressure traverses are shown on Figure 24. Although these traces appear reasonably smooth, it should be recalled that the static-probe resolution is quite poor, since the diameter of the probe was never smaller than five times or so the wake thickness. On the other hand there is strong belief that the mixing in the far wake occurs at constant pressure, or else the whole flow system should shift progressively in the directly of decreasing pressure. In fact, this probe gave seemingly good resolution in regions of sensible pressure gradients, such as at or near shock waves.

Hot-wire measurements consist of the usual four sets: one set consists of five curves at each X station, necessary to complete the inputs for the mean flow measurements. A second set, with 15 curves (each at different current) traces the variation of mean voltage across the wake; a companion set of 15 curves plots the mean-square of the wire a.c. (turbulent) component. Here one should note that the turbulent fluctuations are highest on the side of the wake where the velocity gradients are the highest. Spectral measurements have not been taken as yet.

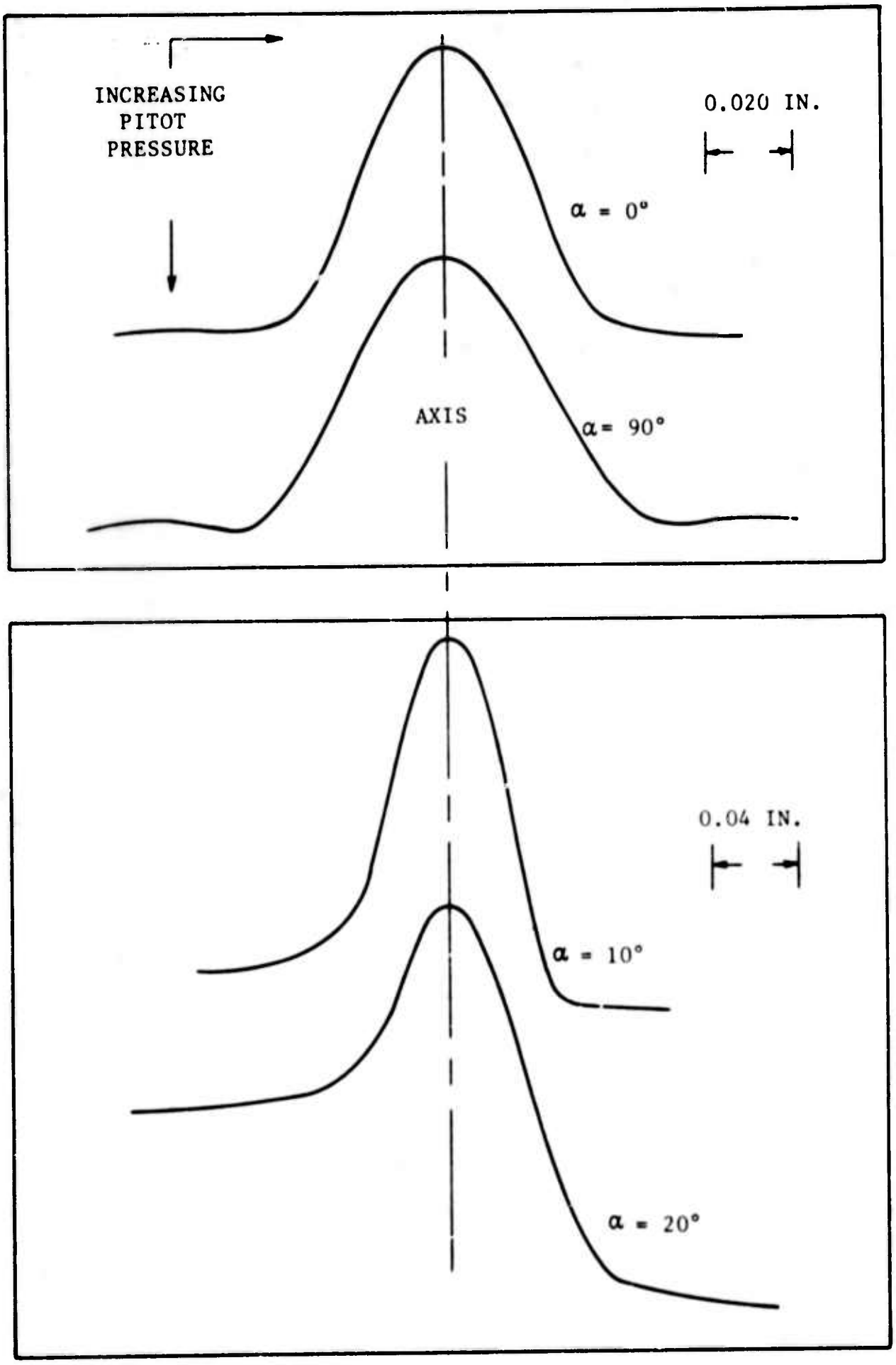

30881 U

FIGURE 23 TYPICAL PITOT-PROBE TRACES OF THE TWO-DIMENSIONAL WAKE AT VARIOUS ANGLES OF ATTACK

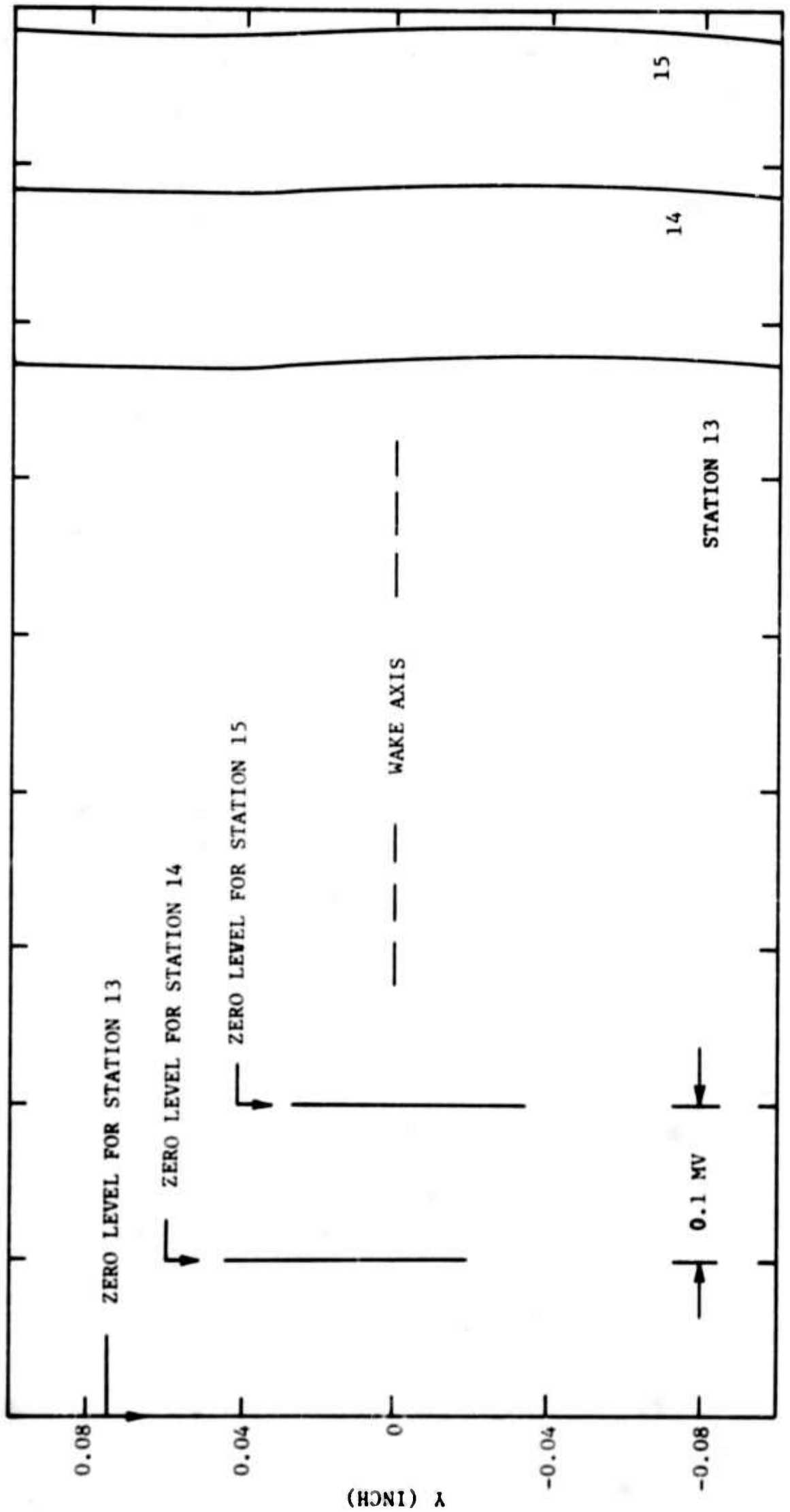

B0882 U

FIGURE 24 TYPICAL STATIC-PROBE TRACES OF THE TWO-DIMENSIONAL WAKE FOR A 20-DEGREE INCIDENCE ANGLE

SECTION V

SUPERSONIC WAKE WITH HEAT TRANSFER

5.1 INTRODUCTION

There are several distinct reasons why the pressure of heat transfer is important to understanding the fluid mechanics of the high-speed wakes. In the first place, it is well known from stability arguments (Reference 14) that the location of wake transition to turbulence is sensitive to heat exchanged between the body and the flow. Secondly, the extent to which heat transfer changes the self-preservation behavior is not well understood. Third, the fluctuations in the wake are much more complex with heat-transfer; for example, the simple relationship between velocity and density fluctuations valid for the isoenergetic wake does not apply.

In the present series of experiments, it is planned to study the mean, intermittent and turbulent flow component behind an axi-symmetric cooled model and a two-dimensional heated model. The latter experiment has been initiated and most of the test have actually been completed. It will be described in this section.

5.2 MODEL AND FACILITIES

This experiment is performed in the same wind-tunnel, at the same conditions, with the same model and concurrently as the angle-of-attach experiment discussed in Section IV. Provisions to the model support, additional to those described in the latter section as necessary for the angle-of-attach measurement, were incorporated specifically for the heat-transfer measurement.

The steel ribbon is heated electrically by a Harrison Laboratories Model No. 814A regulated dc power supply. Load regulation is held to below 0.05 percent, and power-line ripple, already low, is made effectively imperceptible because of high thermal inertia of the heated ribbon. The ribbon current can be adjusted from 0 to 25 amperes dc and is continuously displayed on a Speedomax-W strip-chart recorder running at a speed of 1 inch of paper per second. Aided by the chart resolution and a fine variable resistor added externally to the circuit, the operator can thus readjust and control the ribbon current to about 0.015 percent of the desired value, an error lying much below the current change needed for perceptible changes in the heated wake characteristics. The power settled upon for this measurement will be given farther below.

Expansion of the model by thermal relaxation necessitated a scheme by which the ribbon tension could be adjusted automatically. This was done by spring-loading one end of the ribbon so that the model could expand when heated and retract to a stretched position when the electrical power was turned off.

5.3 ADJUSTMENT OF OPERATING CONDITIONS

To bring about easily observable heat-transfer effects, it was desired to dissipate the highest possible amount of power in the ribbon. Several other conditions should be satisfied simultaneously; the ribbon should not weaken structurally or deform, the turbulence should not be inhibited to the point where the wake became wholly laminar, and the ribbon temperature non-uniformity because of heat conduction into the supports should be kept minimal. There was furthermore some fear that the increased wake temperatures could restrict the operating temperature of the hot-wire or even destroy it when both the model and the hot-wire operating temperatures were high. As it developed, all these criteria were satisfied once the ribbon maximum power was set.

This was accomplished by gradually increasing the ribbon current until the model glowed faintly in the supersonic flow. The current was then reduced until the glow disappeared. At this point the ribbon current was set at 19.90 amperes giving a voltage drop across it of 4.344 volts dc, for a total power dissipation of W = 86.8 watts. It is interesting to compare this power to the "Kinetic" power of the flow P = (drag) x (flow velocity). Utilizing the viscous drag coefficient of the ribbon from the zero-incidence WED experiment (Section II) a ratio of W/P $\doteq$ 1.2 is obtained.

After the necessary tests for finding the true zero-twist and zero-incidence angles (see Reference 1), the hot-wire was employed qualitatively for studying the transition to turbulence with and the transverse (span-wise) uniformity of the heating process. Transition was detected by the usual method of noting the point of maximum turbulence intensity along the center line (Reference 15). Figure 25 shows the remarkable differences in transition distance observed with heating* this distance, located about 100 inches virtual diameters (momentum thicknesses) behind the adiabatic body, moved to about 800 diameters when heating was applied. This phenomenon is consistent with the predictions of stability theory by which the laminar wake is stabilized if the model or vehicle producing it is heated (Reference 14). One result of this transition delay was that the available range in the axial direction over which diagnostics could be made was only about half the range available for wake studies with the adiabatic body. In exchange, however, one obtains a long transitional wake from which information important to the transition process could be extracted. For this reason probings began again, as in WED, shortly downstream of the body rather than at the transition distance.

Visual observation of the ribbon following its overheating to the glowing point showed that its rear half (from about mid-chord to the trailing edge) had been discolored in the way typical of metals after exposure to high temperatures. That the ribbon temperature increases along its chord toward the trailing edge is fully expected because of the more efficient

*Henceforth "heating" refers to the 86.8 watts settled upon as noted previously.

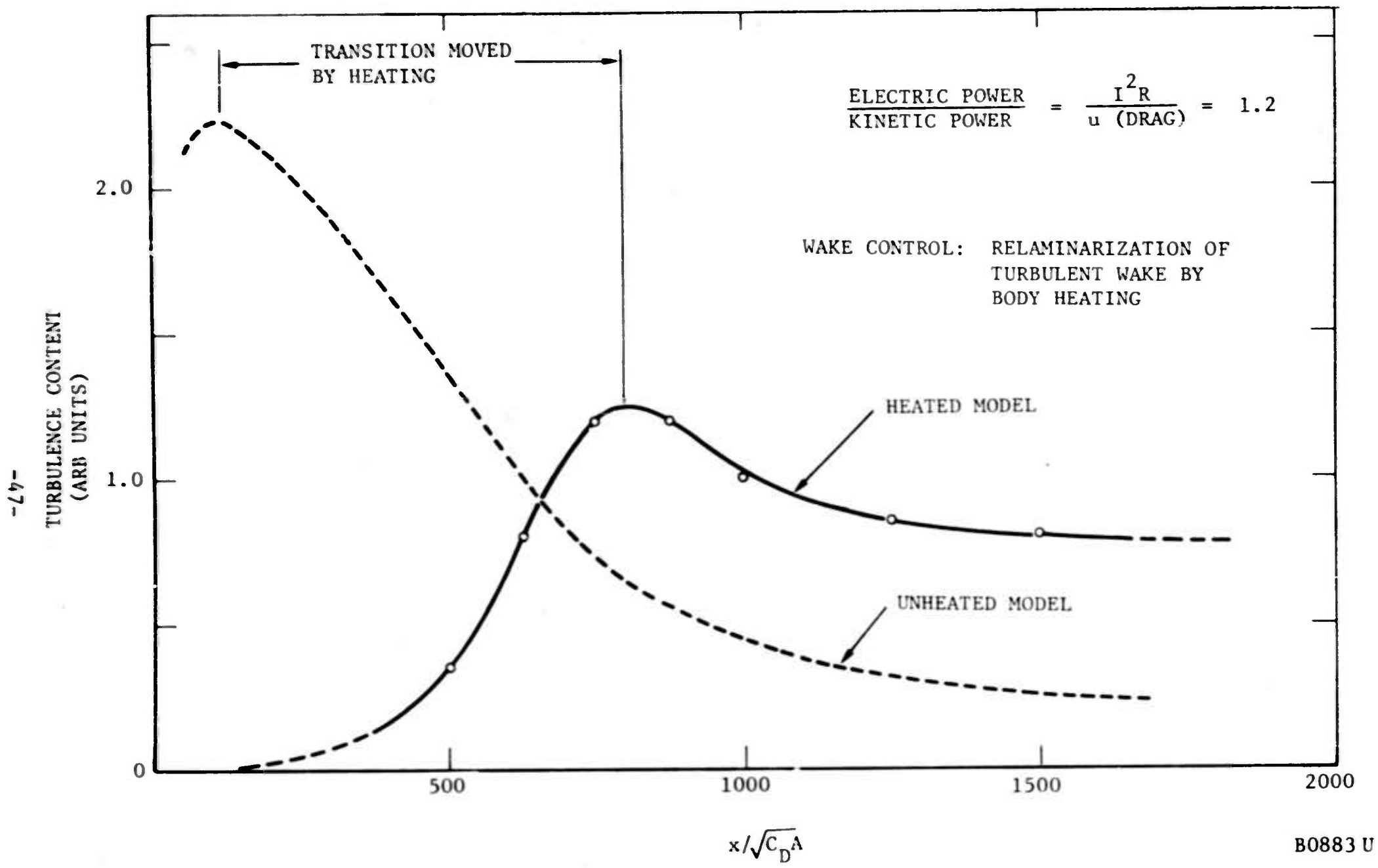

FIGURE 25 DELAY OF TRANSITION TO TURBULENCE IN THE WAKE BROUGHT ABOUT BY HEAT TRANSFER

heat transfer for the thinner boundary layer. The discolored region extended uniformly along the span, but it was observed to stop abruptly about one ribbon chord before it reached the tunnel sidewalls. The ends of the ribbon were therefore cooler since, of course, heat conduction to the solid supports increased at those points.

The observations described above are crucial to the span-wise uniformity of heat transfer from the ribbon to its wake, that is, the question of true two-dimensionality of the experiment. This question was further examined by taking hot-wire profile of the local total wake temperature at fixed distances behind the model and different spanwise stations. Within an inch of the spanwise direction around the center-span position (covering about 35 percent of the total span), the wake axis temperature varied by about 10 percent; at least part of this variation is attributable to slight flow non-uniformities. The two-dimensionality was thus judged to be adequate.

5.4 PROCEDURES AND INSTRUMENTATION

The instrumentation used for this work was identical to that used for the WED and WEF experiments. Although the ribbon itself was heated highly, turbulent diffusion reduced the local stagnation temperatures to the point where no question of damage to the probes by high temperatures ever arose. In fact the 0.00005 inch diameter wire was operated in the same full range of heating currents (maximum of about 7.5 milliamperes) without ever failing by causes attributable to high wake temperatures.

The present experiment, done with the heated two-dimensional body at zero incidence, is designated WEG (Wake Experiment G). The measurements were performed at each of 23 axial positions along the wake. (XSTATIONS 1 through 23) beginning at 0.658 inch from the ribbon mid-chord point. At each station one pitot-pressure transverse, one static-probe transverse, and five hot-wire traverses were performed to collect data sufficient to describe fully the mean flow field. Each wire traverse was of course performed at different heating currents. For the turbulence, 15 traces of mean wire voltage and rms voltage were collected at each station. For the spectra, ten distinct radial locations were chosen at which spectra were recorded at each of six different heating currents. Since the acquisition and reduction of the spectral data is extremely time-consuming, data were taken only at alternate XSTATIONS (the odd-numbered stations 1, 3, 5,...23). Thus a total of 10 x 6 x 12 = 720 spectra were recorded.

It is perhaps advisable to reiterate here the data reduction process through which the WEG data are now progressing. The mean-flow data are digitized and put into the WEB-V and WEB-VIII computer programs which have for some time been prepared for the Philco-2000 digital computer.

The spectral data are first used into the WEB-II program from which one extracts the so-called error ratios, that is, a correction factor necessary to use in correcting the system frequency response. The output of this program and the turbulence data are then used into the WEB-III and WEB-IV programs to deduce the turbulence properties and further into the WEB-VII program from which turbulence properties in scaled form are obtained.

5.5 RESULTS TO DATE

The raw data obtained to date give the following indications of wake behavior:

(1) Profiles are symmetric as expected. This applies equally to the pilot, static and hot-wire data.

(2) As expected when heat transfer is at play, the flow profiles at the far wake positions stand out much more clearly than in the adiabatic experiment. The local total temperature, especially, barely distinguishable from the free-stream value in WED, has an outstanding intensity.

(3) The turbulence intensity increases at anv given station following transition.

(4) The spectra again show the energy prominence they also displayed in WED; the peak, however, is displaced to lower frequencies, perhaps reflecting an overall thickening of the wake.

APPENDIX I

DATA-HANDLING PROCEDURES

1.1 INTRODUCTION

In the work done on the turbulent wake structure by this company in the recent past, it has been demonstrated that automated procedures in the wind-tunnel have enabled a very great volume of relevant data to be acquired. It is necessary to accelerate the reduction rate of these data between the point of transducer output and the point of input into the computer. Furthermore, it is clear that the present hot-wire anemometer system ought to be improved to handle higher frequency ranges. Finally, it is necessary to re-direct the experimental equipment for near-future requirements involving novel measurements of turbulence. Considerable effort has been put into the planning of new data-producing and handling techniques.

1.2 DATA ACQUISITION: HOT-WIRE ANEMOMETRY

As Paragraph 2.4 explains, the present hot-wire anemometer system is capable of yielding data to frequencies of order 1MHz. A new system is being planned to extend this range to several MHz. This system is based on the use of an extremely fine hot-wire, 0.00001 inches in diameter, and about 0.002 inches long. The time-constant of this wire, unaided by electronic compensation, will be between 10 and 20 microseconds. The wire signal will be directed into a new constant-current hot-wire amplifier which has now been designed. This amplifier will utilize modest amplification ratios and a floor-to-ceiling ratio not much in excess of 500. Solid-state amplifiers in several stages will produce a flat straight-amplifier response to beyond 1 MHz and a compensation capability in excess of that frequency. Self-contained mercury-cell power supplies will heat the wire. Two such amplifiers are being planned.

The next element in the line will be a high-frequency-response (2 MHz or better) magnetic tape recorder with a minimum of seven channels, any number of which will be preselected to accept dc signals, with the remainder used for the high-frequency ac signals. The recorder will be used for a variety of important functions. In a typical wake experiment two ac channels will carry the direct hot-wire output (the second channel being active, for example, in correlation measurements with two wires), two dc channels will be carrying voltages proportional to two position coordinates, and the remaining three dc channels the wire rms output, wire mean voltage and wire current. By recording at closely-spaced points and different wire currents, it is hoped to obtain a complete record of an entire experiment stored in two 15 inch reels of magnetic tape.

The signals most time consuming operation in the current work, both as regards the data acquisition and its digitization, is the measurement of spectra. Currently, several hundred spectra are obtained for each experiment. Each spectrum is obtained in analog, bivariate form and then digitized by hand for key-punching into computer card format. It is planned to bypass this operation by taking the ac signal from the magnetic tape, digitizing

it electromechanically and computing its spectrum by using a computer program (the "Fast Fourier Transform" program).

The remainder of the operations needed for mean and turbulence measurements involve only dc measurements e.g., a dc transducer output voltage and a dc position voltage which can be obtained by either of three methods: (1) from the points of the magnetic-tape file of the complete experiment (2) by a second file easily made by repeating the experiment by continuous traverses, or (3) by a method identical to (2) but where the two voltages are digitized and punched (on paper tape or cards) in real time without recourse to magnetic tape. In either case large savings in time are possible.

REFERENCES

1. Advanced Penetration Problems, Task 2: Wake Structure Measurements, Report Number UG-4201, Philco-Ford Corporation, Newport Beach, California, 15 October 1967.

2. Demetriades, A., Mean Flow Measurements In An Axisymmetric Compressible Turbulent Wake, Report Number U-3978, Philco-Ford Corporation, Newport Beach, California, 1 March 1967.

3. Lanfer, J., On Turbulent Shear Flows of Variable Density, AIAA Paper Number 68-41, 6th Aerospace Science Meeting, New York, New York, January 1968.

4. Townsend, A.A., The Structure of Turbulent Shear Flow, Cambridge University Press, 1956.

5. Demetriades, A., Turbulent Front Structure of An Axisymmetric Compressible Wake, Report Number UG-4259, Philco-Ford Corporation Newport Beach, California, 15 November 1967.

6. Demetriades, A., Turbulence Measurements In An Axi-symmetric Compressible Wake, Report Number UG-4118, Philco-Ford Corporation, Newport Beach, California, 1 August 1967.

7. Becker, H., Hottel, H.C. and Williams, G. C., The Nozzle-Fluid Concentration Field of the Round, Turbulent Free Jet, Journal of Fluid Mechanics, Volume 30, Part 2, p.285, 1967.

8. Bradbury, L.J.S., A Simple Circuit For The Measurement of The Intermittency Factor In A Turbulent Flow, Aeronautical Quarterly, Volume 15, p.281, 1965.

9. Corrsin, S. and Kistler, A. L., Free-Stream Boundaries of Turbulent Flows, NACA TR 1244, Washington, D.C., 1953.

10. Proudian, A. P. and Feldman, S., A New Model For Mixing and Fluctuations In A Turbulent Wake, AIAA Journal, Volume 3, Number 4, p.602, April 1965.

11. Lin, S. C. and Hayes, J. E., A Quasi-One-Dimensional Treatment of Chemical Reactions In Turbulent Wakes of Hypersonic Objects, AIAA Journal, Volume 2, Number 7, p.1214, July 1964.

12. Demetriades, A., Electron Fluctuations In An Equilibrium Turbulent Plasma, AIAA Journal, Volume 2, Number 7, p.1347, July 1964.

13. Demetriades, A., and Von Seggern, L., Design, Performance and Operation of the Mach 3 Wind-Tunnel, Report Number U-3390, Philco-Ford Corporation, Newport Beach, California, 15 November 1965.

14. Lees, L and Gold, H., Stability of Laminar Boundary-Layers and Wakes At Hypersonic Speeds, Proceedings of International Symposium on Fundamental Phenomena In Hypersonic Flow, Cornell University Press, 1966.

15. Demetriades, A., Some Hot-Wire Anemometer Measurements In A Hypersonic Wake, Heat Transfer and Fluid Mechanics Institute Proceedings, Stanford University Press., 1961, p.1.

Unclassified

Security Classification

DOCUMENT CONTROL DATA · R&D

(Security classification of title, body of abstract and indexing annotation must be entered when the overall report is classified)

1 ORIGINATING ACTIVITY (Corporate author)
Philco-Ford Corporation, Space and Re-entry Systems Division

2a REPORT SECURITY CLASSIFICATION
Unclassified

2b GROUP
N/A

3 REPORT TITLE
Advanced Penetration Problems, Wake Structure Measurements

4 DESCRIPTIVE NOTES (Type of report and inclusive dates)
Semiannual, 16 October 1967 through 15 April 1968

5 AUTHOR(S) (Last name, first name, initial)
Demetriades, A.

6 REPORT DATE	7a TOTAL NO OF PAGES	7b NO OF REFS
15 May 1968	63	15

8a CONTRACT OR GRANT NO.
F04701-68-C-0032

b PROJECT NO.
ARPA Order 888

c

d

9a ORIGINATOR'S REPORT NUMBER(S)

9b OTHER REPORT NO(S) (Any other numbers that may be assigned this report)
SAMSO TR-68-362 Vol. II

10 AVAILABILITY/LIMITATION NOTICES
This document may be further distributed by any holder only with specific approval of SAMSO (SMSD), [redacted]

11 SUPPLEMENTARY NOTES

12 SPONSORING MILITARY ACTIVITY
SMSO
Norton Air Force Base
California

13 ABSTRACT

Progress on the subject contract in the period October 15, 1967 to April 15, 1968 is described in this report. Work has been performed on the turbulent structure of a two-dimensional supersonic wake at angle of attack, on a similar wake at zero incidence but with heat transfer, and a turbulent plasma jet. Data from a zero-incidence, adiabatic wake are being further reduced. Notable findings in these experiments include highly accurate values of the turbulent Reynolds and Prandtl number, a re-appearance of the so-called front wavelength of free turbulence, and the explanation of very large electron density fluctuations as due to transitional mixing.

DD FORM 1 JAN 64 1473

Unclassified

Security Classification

14 KEY WORDS	LINK A ROLE	LINK A WT	LINK B ROLE	LINK B WT	LINK C ROLE	LINK C WT
Wake						
Jet						
Plasma						
Turbulence						
Supersonic						
Intermittency						
Angle of attack						
Heat Transfer						
Transition						
Fluctuations						
Electron Density						
Similarity						
Self-preservation						

INSTRUCTIONS

1. ORIGINATING ACTIVITY: Enter the name and address of the contractor, subcontractor, grantee, Department of Defense activity or other organization *(corporate author)* issuing the report.

2a. REPORT SECURITY CLASSIFICATION: Enter the overall security classification of the report. Indicate whether "Restricted Data" is included. Marking is to be in accordance with appropriate security regulations.

2b. GROUP: Automatic downgrading is specified in DoD Directive 5200.10 and Armed Forces Industrial Manual. Enter the group number. Also, when applicable, show that optional markings have been used for Group 3 and Group 4 as authorized.

3. REPORT TITLE: Enter the complete report title in all capital letters. Titles in all cases should be unclassified. If a meaningful title cannot be selected without classification, show title classification in all capitals in parenthesis immediately following the title.

4. DESCRIPTIVE NOTES: If appropriate, enter the type of report, e.g., interim, progress, summary, annual, or final. Give the inclusive dates when a specific reporting period is covered.

5. AUTHOR(S): Enter the name(s) of author(s) as shown on or in the report. Enter last name, first name, middle initial. If military, show rank and branch of service. The name of the principal author is an absolute minimum requirement.

6. REPORT DATE: Enter the date of the report as day, month, year; or month, year. If more than one date appears on the report, use date of publication.

7a. TOTAL NUMBER OF PAGES: The total page count should follow normal pagination procedures, i.e., enter the number of pages containing information.

7b. NUMBER OF REFERENCES: Enter the total number of references cited in the report.

8a. CONTRACT OR GRANT NUMBER: If appropriate, enter the applicable number of the contract or grant under which the report was written.

8b, 8c, & 8d. PROJECT NUMBER: Enter the appropriate military department identification, such as project number, subproject number, system numbers, task number, etc.

9a. ORIGINATOR'S REPORT NUMBER(S): Enter the official report number by which the document will be identified and controlled by the originating activity. This number must be unique to this report.

9b. OTHER REPORT NUMBER(S): If the report has been assigned any other report numbers *(either by the originator or by the sponsor)*, also enter this number(s).

10. AVAILABILITY/LIMITATION NOTICES: Enter any limitations on further dissemination of the report, other than those imposed by security classification, using standard statements such as:

(1) "Qualified requesters may obtain copies of this report from DDC."

(2) "Foreign announcement and dissemination of this report by DDC is not authorized."

(3) "U. S. Government agencies may obtain copies of this report directly from DDC. Other qualified DDC users shall request through _____."

(4) "U. S. military agencies may obtain copies of this report directly from DDC. Other qualified users shall request through _____."

(5) "All distribution of this report is controlled. Qualified DDC users shall request through _____."

If the report has been furnished to the Office of Technical Services, Department of Commerce, for sale to the public, indicate this fact and enter the price, if known.

11. SUPPLEMENTARY NOTES: Use for additional explanatory notes.

12. SPONSORING MILITARY ACTIVITY: Enter the name of the departmental project office or laboratory sponsoring *(paying for)* the research and development. Include address.

13. ABSTRACT: Enter an abstract giving a brief and factual summary of the document indicative of the report, even though it may also appear elsewhere in the body of the technical report. If additional space is required, a continuation sheet shall be attached.

It is highly desirable that the abstract of classified reports be unclassified. Each paragraph of the abstract shall end with an indication of the military security classification of the information in the paragraph, represented as *(TS), (S), (C), or (U)*

There is no limitation on the length of the abstract. However, the suggested length is from 150 to 225 words.

14. KEY WORDS: Key words are technically meaningful terms or short phrases that characterize a report and may be used as index entries for cataloging the report. Key words must be selected so that no security classification is required. Identifiers, such as equipment model designation, trade name, military project code name, geographic location, may be used as key words but will be followed by an indication of technical context. The assignment of links, rules, and weights is optional

GPO 866-551